Roles of CBP7 and Rap Proteins in *Dictyostelium* Cell Migration and Development

조선대학교 대학원

생명과학과

박 병 규

Roles of CBP7 and Rap Proteins in *Dictyostelium* Cell Migration and Development

Dictyostelium 세포이동과 발생과정에서의 CBP7과 **Rap** 단백질들의 역할

2018 년 2 월 23 일

조선대학교 대학원

생명과학과

박 병 규

Roles of CBP7 and Rap Proteins in *Dictyostelium* Cell Migration and Development

지도교수　　전 택 중

이 논문을 이학석사학위 신청 논문으로 제출함

2017 년 10월

조선대학교 대학원

생명과학과

박　병　규

박병규의 석사학위논문을 인준함

위원장 조선대학교 부교수 이 준 식 (인)

위 원 조선대학교 부교수 조 광 원 (인)

위 원 조선대학교 부교수 전 택 중 (인)

2017년 11월

조선대학교 대학원

CONTENTS

i

PART II. Roles of Rap Proteins in *Dictyostelium*

Cell Migration and Development

LIST OF TABLES

LIST OF FIGURES

ABBREVIATIONS

cAMP	**Cyclic adenosine monophosphate**
CBP	**Calcium binding protein**
Fluo4-AM	**Non-fluorescent acetoxymethyl ester**
GAP	**GTPase activating proteins**
GDP	**Guanosine diphosphate**
GEF	**Guanine nucleotide exchange factor**
GFP	**Green fluorescent protein**
GPCR	**G-protein coupled receptor**
GTP	**Guanosine triphosphate**
PBS	**Phosphate-buggered saline**
PCR	**Polymerase chain reaction**
PH	**Pleckstrin homology**
PI	**Propidium iodied**
PI3K	**Phosphatidylinositol 3-kinase**
RFP	**Red fluorescent protein**
SD	**Standard deviation**
SEM	**Standard error of measurement**

ABSTRACT

Roles of CBP7 and Rap Proteins in *Dictyostelium* Cell Migration and Development

Byeonggyu Park

Advisor: Associate Prof. Taeck Joong Jeon, Ph.D.

Department of Life Science,

Graduate School of Chosun University

Calcium ions are involved in the regulation of diverse cellular processes. Fourteen genes encoding calcium binding proteins have been identified in *Dictyostelium*. CBP7, one of the 14 CBPs, is composed of 169 amino acids and contains four EF-hand motifs. Here, I investigated the roles of CBP7 in the development and cell migration of *Dictyostelium* cell and found that high levels of CBP7 exerted a negative effect on cells aggregation during development, possibly by inhibiting chemoattractant-directed cell migration. While cells lacking CBP7 exhibited normal development and chemotaxis similar that of wild-type cells, CBP7 overexpressing cells completely lost their chemotactic abilities to move toward increasing cAMP concentrations. This resulted in inhibition of cellular aggregation, a process required for forming multicellular organisms during development. Low levels of cytosolic free calcium were observed in CBP7 overexpressing cells, which was likely the underlying cause of their lack of chemotaxis. These results demonstrate that CBP7 plays an important role in cell spreading and cell-substrate adhesion. *cbp7* null cells showed decreased cell size and cell-substrate adhesion. In addition, experiments using point-mutated CBP7 cells showed that all EF-hand domain of CBP7 was important for CBP7 to function in the developmental process. Yeast two-hybrid experiments using CBP7 as a bait showed

1

that CBP7 specifically binds to activation RasG. These results suggest that CBP7 has important roles in the development process through all of CBP7 EF-hand domains and by binding to RasG. The present study contributes to further understanding the role of calcium signaling in regulation of cell migration and development and the relationship between the calcium signaling and Ras signaling pathways.

Ras proteins are small, monomeric GTPases that act as crucial regulators of a number of cellular signaling pathways, including proliferation, cell migration, differentiation, and apoptosis. The functions of most of these Ras proteins in development and cell migration have not been studied yet. Therefore, I investigated the roles of RapB and RapC in cell migration and development. RapB and RapC has the highest homology (86.6%, 50.9 % amino acid identity) with Rap1, which is a key regulator in cell adhesion and cell migration. To investigate the functions of RapB, I prepared constitutively active form of GFP-RapB cells (GFP-RapB ^{G31V} cells) and dominantly negative form of GFP-RapB cells (GFP-RapB^{S36N} cells). I found that GFP-RapB^{S36N} cells displayed decreased cell size and weak cell-substrate adhesion than wild-type cells. These results demonstrate that RapB positive plays cell spreading and cell-substrate adhesion. In addition, I investigated the roles of RapB in the development and cell migration of *Dictyostelium* cells and found that GFP-RapB ^{G31V} cells exerted late development, possibly through strong cell-substrate adhesion appeared inhibition of chemoattractant-mediated cell migration in development. These results demonstrate that RapB negative plays in cell migration and development.

To investigate the functions of RapC, I prepared *rapC* null cells by homologous recombination. Unexpectedly, RapC might have opposite functions to Rap1 and RapB. *rapC* null cells showed flattened and spread morphology and strong cell-substrate adhesion compared to wild-type cells. The results demonstrate that RapC plays an important negative role in cell spreading and cell-substrate adhesion as opposed to Rap1 and RapB. In addition, *rapC* null cells had a cytokinesis defect. These phenotypes of *rapC* null cells were rescued

2

by overexpressing GFP-RapC, suggesting that RapC is required for cytokinesis. I investigated the roles of RapC in the development and cell migration of *Dictyostelium* cells and found that *rapC* null cells exerted a negative effect on cells aggregation and fruiting body formation during development, possibly through strong cell-substrate adhesion appeared inhibition of chemoattractant-mediated cell migration and electrical stimulation in development. These results demonstrate that RapC plays an important positive role in cell migration and development as opposed to Rap1 and RapB. The localization assay showed that RapB and RapC localized to the cell plasma membrane and preferentially at the leading edge in migrating cells. The present study contributes to our understanding of the molecular mechanism of Rap proteins that regulates cytoskeletal rearrangement and morphogenesis in *Dictyostelium*

PART Ⅰ. CBP7 Interferes with the Multicellular Development of *Dictyostelium* by Inhibiting Chemoattractant-Mediated Cell Aggregation

I. Introduction

Calcium ions are involved in the regulation of diverse cellular processes such as chemotaxis, cell adhesion, and muticellular development (Clapham, 2007; Lusche *et al.*, 2009; Siu *et al.*, 2011). Calcium ions regulate cellular processes though their interactions with calcium-binding proteins (CBPs). Calcium-binding proteins function as calcium buffers to control the intracellular concentration of calcium ions or as calcium sensors to transduce signals to a series of downstream effectors (Chin and Means, 2000; Clapham, 2007).

Dictyostelium discoideum is a unicellular eukaryotic microorganism used as a model system to address many important cellular processes including cell migration, cell division, phagocytosis, and development (Chisholm and Firtel, 2004; Siu, Sriskanthadevan et al., 2011; Lee and Jeon, 2012). Upon starvation, *Dictyostelium* initiates a multicellular developmental process by forming aggregates, slugs, and finally, fruiting bodies. In the initial stages of this developmental process, *Dictyostelium* cells emit the chemoattractant, cAMP, which cause cells to migrate in the direction of increasing concentrations along the gradient to form aggregates (Chisholm and Firtel, 2004). It has been shown that the rate of Ca^{2+} influx was stimulated by the chemoattractant, cAMP, and that the intracellular calcium ions affected cell-cell adhesion and cell fate determination (Malchow *et al.*, 1996; Yumura *et al.*, 1996; Chisholm and Firtel, 2004).

4

Fourteen calcium-binding proteins (CBP) have been identified in *Dictyostelium*. The expressions of these proteins are tightly linked to their multicellular stages of development. CBP1 is expressed prior to cell aggregation and associates with the actin cytoskeleton. CBP1 is suggested to regulate the reorganization of the actin cytoskeleton during cell aggregation (Dharamsi *et al.*, 2000; Dorywalska *et al.*, 2000; Sakamoto *et al.*, 2003). *cbp1* null cells showed delayed aggregation and development (Dharamsi, Tessarolo et al., 2000). CBP1 also interacts with another calcium-binding protein, CBP4a, and the actin-binding proteins, protovillin and EF-1a, in yeast two-hybrid experiments (Dorywalska, Coukell et al., 2000). The function of CBP2 is unknown, but its mRNA concentrations was shown to peak during cellular aggregation and then decrease after 12 h, suggesting that it specifically functions during distinct stages of development (Andre *et al.*, 1996). CBP3 is relatively well studied, and actin 8 was identified as an interacting protein with CBP3 in yeast two-hybrid screening. Cells overexpressing CBP3 showed accelerated cell aggregation and increased number of small aggregates and fruiting body. It was suggested that CBP3 interacts with the actin cytoskeleton and plays important roles in cell aggregation and slug migration during development (Lee *et al.*, 2005; Mishig-Ochiriin *et al.*, 2005). CBP4a is a nucleolar protein that interacts with nucleomorphin, which is a cell cycle checkpoint protein, in Ca^{2+}-dependent manner. CBP4a was suggested to function during mitosis (Myre and O'Day, 2004; Catalano and O'Day, 2013). CBP5, 6, 7, and 8 contain canonical EF-hand motifs, which mediate their Ca^{2+}-binding properties. These proteins are under spatial and temporal regulation during development and might have specific roles in cellular processes such as cell migration, cell adhesion, and development (Sakamoto, Nishio et al., 2003). However, the exact functions of these proteins remain unknown.

Here, I investigated the functions of CBP7, one of the CBP proteins, in cell migration and development by examining the characteristics of cells lacking or overexpressing CBP7.

II. Materials and Methods

II-1. Cell culture

Dictyostelium wild-type KAx-3 cells were cultured axenically in HL5 medium or in association with *Klebsiella aerogenes* at 22°C. The knock-out strains and transformants were maintained in 10 μg/ml blasticidin or 10 μg/ml of G418.

II-2. Strains, and plasmid construction

The full coding sequence of *cbp7* cDNA was generated by reverse transcription polymerase chain reaction (RT-PCR) and cloned into the *Eco*RI – *Xho*I site of the expression vector pEXP-4(+) containing a GFP fragment. The plasmids were transformed into KAx-3 cells or *cbp7* null cells. The *cbp7* knockout construct was made by inserting the blasticidin resistance cassette (*bsr*) into *Bgl*II site created at nucleotide 415 of *cbp7* gDNA and used for a gene replacement in KAx-3 parental strains. Randomly selected clones were screened for a gene disruption by PCR. The primers used in the screening for a gene replacement are following (Table 1). Expression mutants, CBP7(N24A, D26A), CBP7(D63, 65A), CBP7(D107, 109A), and CBP7(D142, 144A), the various mutation *cbp7* sequences were amplified by PCR using site-directed mutagenesis (Table 1) and cloned into the *Eco*RI – *Xho*I site of the expression vector pEXP-4(+) containing a GFP fragment.

II-3. Cell adhesion assay

Cell adhesion assay was performed as described previously (Mun *et al.*, 2014). Log-phase growing cells on the plates were washed and resuspended at a density of 2×10^6 cells/ml in 12 mM Na/K phosphate buffer. 200 μl of the cells were placed and attached on the 6-well culture dishes. Before shaking the plates, the cells were photographed and

6

counted for calculating the total cell number. To detach the cells from the plates, the plates were constantly shaken at 150 rpm for 1h, and then the attached cells were photographed and counted (attached cells) after the medium containing the detached cells was removed. Cell adhesion was presented as a percentage of attached cells compared with total cells.

II-4. Development assay

Development was performed as described previously (Jeon *et al.*, 2009). Exponentially growing cells were harvested and washed twice with 12 mM Na/K phosphate buffer (pH 6.1) and resuspended at a density of 3.5×10^7 cells/ml. 50 μl of the cells were placed on Na/K phosphate agar plates and developed for 24 h. For development of the cells under submerged conditions, exponentially growing cells (2×10^6 cells) were placed and developed in 12-well plates containing Na/K phosphate buffer. The muticellular developmental organisms was photographed and examined with a phase-contrast microscope at the indicated times in the figures.

II-5. Chemotaxis assay

Chemotaxis towards cAMP was examined as described previously (Jeon *et al.*, 2007b; Mun, Lee et al., 2014). The aggregation-competent cells were prepared by incubating the cells at a density of 5×10^6 cells/ml in Na/K phosphate buffer for 10 h. Cell migration was analyzed using a Dunn Chemotaxis Chamber (Hawksley). The images of chemotaxing cells were taken at time-lapse intervals of 6 s for 30 min using an inverted microscope (IX71; Olympus). The data were analyzed using the NIS-Elements software (Nikon) and Image J software (National Institures of Health). For examining cell migration in the aggregation stage of development, 2.5% of RFP-labeled wild-type cells and 2.5% of cells expressing GFP-CBP7 were mixed with 95% of unlabeled wild-type cells and developed on Na/K phosphate agar plates. The fluorescence images of moving cells at the aggregation step of

development were captured by the NIS-Elements software, and the movement of fluorescent cells was traced and analyzed using the Image J software. 'Trajectory speed' was used to quantify motility of the cells. The trajectory speed is the total distance travelled of a cell divided by time. 'Directionality' is a measure of how straight the cells move. Cells moving in a straight line have a directionality of 1. It was calculated as the distance moved over the linear distance between the start and the finish.

II-6. Measurement of cytosolic calcium

Fluo-4 AM, a fluo calcium indicator, was obtained from Molecular Probes, and the cells were labeled with fluo-4 AM according to the protocol provided by manufactures. *Dictyostelium* cells at a density of 5×10^6 cells/ml in 1 x PBS buffer were added by 2.2 mM Fluo-4 AM (final concentration, 8 μM). The mixed solutions were transferred into 96-well plates and incubated in the dark at room temperature for 60 min, followed by washing gently twice with 1 x PBS buffer. The fluorescence levels of the cells in the wells were quantified using a fluorescence microplate reader (Molecular Devices) and SoftMax Pro software. The excitation and emission wavelengths were 494 nm and 506 nm, respectively.

II-7. RT-PCR

The total RNAs from wild-type cells and *cbp7* null cells were extracted by using the SV Total RNA Isolation system (Promega), and the cDNAs were synthesized by reverse transcription with MMLV reverse transcriptase (Promega) using random hexamers and 5 μg of total RNAs. 5μL of the cDNAs were used in the following PCR with 35 cycles employing gene-specific primers. The universal 18S ribosomal RNA specific primers were used as an internal control (Jeon *et al.*, 2007a).

8

II-8. Yeast two-hybrid analysis

The Gal4 yeast two-hybrid screening was used to detect protein-protein interactions. The yeast strain EGY48. The *Dictyostelium ras* cDNA was cloned into the *Eco*RI/*Xho*I site of the Gal4 activation domain (AD) vector pEG202. The *Dictyostelium* cDNA library was cloned into the *Eco*RI/*Xho*I site of the Gal4 DNA binding domain (DBD) vector pJG4-55 to obtain pJG–CBP7. Transformants were selected in a minimal medium lacking uracil, histidine, and tryptophan. The AD plasmid of pEG-Ras and DBD plasmid of pJG–CBP7 were co-transformed into yeast strain EGY48 and assayed for β-galactosidase activity. pJG–RA1 was used as a positive control for RasG interactions.

II-9. Pull-down assay

Log-phase vegetative cells on the plates were washed twice and resuspended at a density of 1×10^7 cells/ml in Na/K buffer. The cells were collected and lysed by mixing with 400μl 1 × lysis buffer(100 mM Tris, pH 7.5, 300 mM NaCl, 50 mM $MgCl_2$, 20% glycerol, 1% NP-40, 2mM DDT, 2 mM vandate, protein inhibitor cocktail). The lysates were centrifuged for 20min, and the supernatants were incubated with 10 μg GST-CBP7 on glutathione-Sepharose beads at 4°C for 2h. The beads were washed two times and subjected to SDS-PAGE and Western blot analysis with an anti-GFP pAb. For control of the input amount, 30 μg of the cells were taken right agter lysis of the cells.

Table 1. PCR primers sequences used for CBP7 study

Gene name	primer	Sequence (5´ → 3´)
18s rRNA	18s rRNA - F	GTAATTCCAGCTCCAATAGC
	18s rRNA - R	GAACGGCCATGCACCAC
CBP7 knock out primer	Ⅰ	GAATTCATGAGCACTTGTGGTGATAATAG
	Ⅱ	CTCGATAGTCTCAGCATTTTGTTCAATTTG
	Ⅲ	CTCGATTTAACAAATTGGACCTCTTGC
	Ⅳ	GATTAATGTGGTATTTTGTCCCAAGAG
CBP7 mutation primer	EF1 mutation - F	GACTTGATAAAGCTAAGGCT AAAAAATTAAACAAAACAG
	EF1 mutation - R	CTGTTTTGTTTAATTTTTTA GCCTTAGCTTTATCAAGTC
	EF2 mutation - F	CTTAAAATTATTGATTTGTC TAAAGCTGGATATGTTTCC
	EF2 mutation - R	GGAAACATATCCAGGTTTA GCCAAATCAATAATTTTAAG
	EF3 mutation - F	GTTCAACAGTTGATATGG CTAATGCTGGTAAATTCAG
	EF3 mutation - R	CTGAATTTACCAGCATTAG CCATATCAACTGTTGAAC
	EF4 mutation - F	CCAAGATTATGAATTAGCTA AGGCTTACAGTGTAACTTC
	EF4 mutation - R	GAAGTTACACTGTAAGCCT TAGCTAAGTCATAATCTTGG

F - forward, R - reverse

10

III. Results

III-1. CBP7, a calcium-binding protein

There are 14 genes encoding CBP proteins in the genomes of *Dictyostelium*. The putative domain structures are depicted (Fig. 1A). Most of the CBP proteins (CBP 1−8 and CBP12) have similar numbers of residues and 4 EF-hand motifs. CBP9 and 14 have three EF-hand motifs. Among them, only CBP1, CBP2, CBP3, CBP4a, and CBP4b have been previously characterized. Here, I investigated one of the 14 CBP proteins, CBP7. *Dictyostelium* CBP7 has 169 amino acids (expected molecular mass of 19.3kDa) and 4 EF-hand motifs (Fig. 1A). The phylogenetic trees of the CBP proteins containing four EF-hand motifs illustrate that CBP7 is closely related to the CBP3, 6, and 12 (Fig. 1C). A multiple alignment of CBP7 with other CBP proteins shows that CBP7 has 74%, 70%, and 68% amino acid identities with CBP6, CBP12, and CBP3, respectively, and contains the conserved residues in all 4 EF-hands that are necessary for calcium binding (Fig. 2). CBP7 is known as a real Ca^{2+}-binding protein (Sakamoto, Nishio et al., 2003).

11
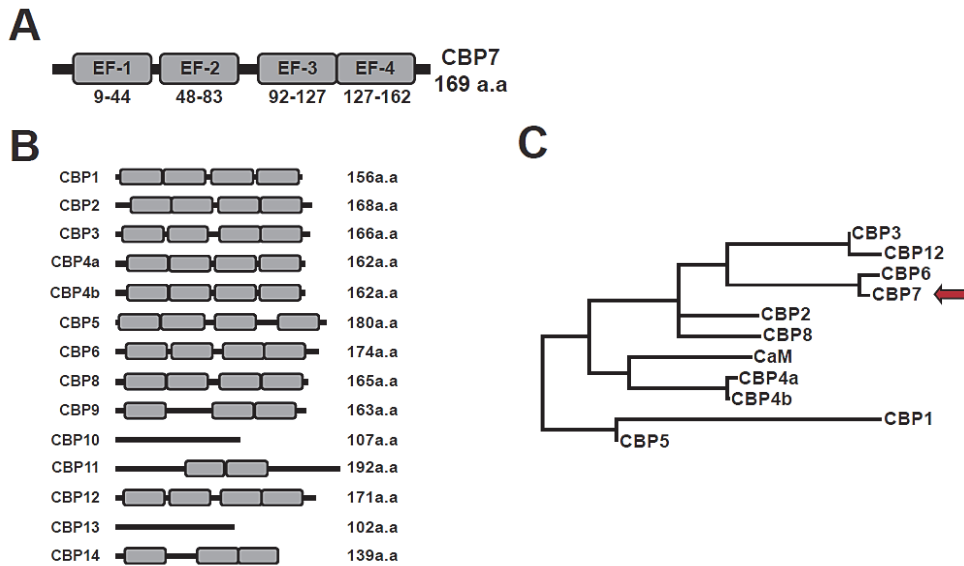
F i g u r e 1 . Domain structure and phylogenetic tree of CBP proteins in *Dictyostelium.*
(A) Domain structure of CBP7 showing four EF-hand motifs. (B) Domain structures of 15 CBPs in *Dictyostelium*. A box indicates an EF-hand motif. (C) Phylogenetic tree analysis of CBPs. The amino acid sequence of CBP7 was compared with those of other CBP proteins. The amino acid sequences of CBPs are available at dictyBase (http://www.dictybase.org. *Dictyostelium discoideum* CBP1 (G0276759); CBP2, (G0267456); CBP3, (G0283613); CBP4a, (G0283153); CBP4b, (G0283083); CBP5 (G0274099); CBP6, (G0283611); CBP7, (G0283609); CBP8, (G0288623); CBP9 (G0272827); CBP10 (G0270210); CBP11 (G0274359); CBP12, (G0283645); CBP13 (G0286371); CBP14 (G0285265); Calmodulin (G0279407).

12
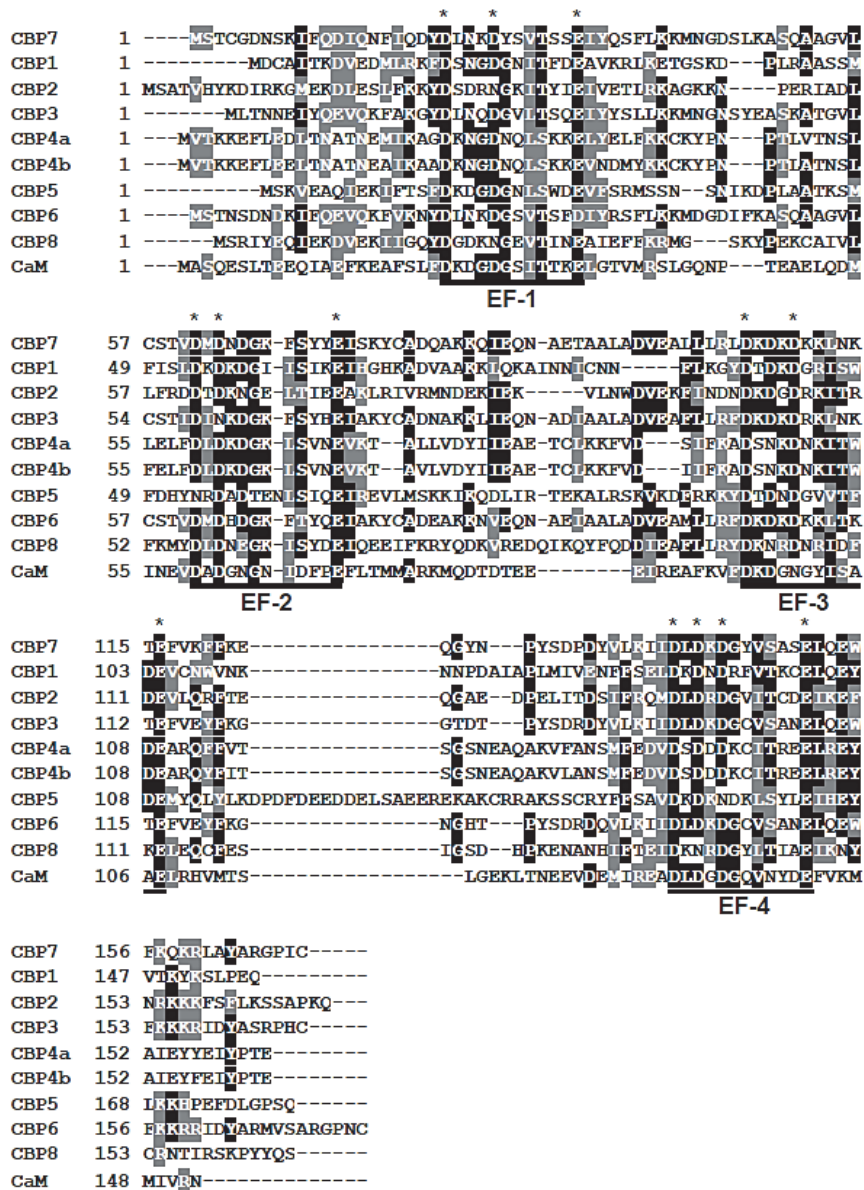
Figure 2. Multiple alignment of CBP proteins.

The amino acid sequence of CBP7 was compared with those of other CBPs containing four EF-hand motifs, which were underlined and marked as EF-1, 2, 3, and 4. The identical residues were highlighted in dark gray or light grey. The conserved residues in the EF-hands were marked with asterisks.

13

To investigate the functions of CBP7, I prepared *cbp7* knock-out strains by homologous recombination with the *cbp7* knock-out DNA construct containing a blasticidin resistance (*bsr*) antibiotic cassette into the *cbp7* genomic DNA of KAx-3 parental strains (Fig. 3A). *cbp7* knock-out cells were confirmed by polymerase chain reactions (PCR) (Fig. 3B). PCR with a set of primers, I/II and I/IV, produced bands of 361 and 826 bp in wild-type cells and bands of 361 and 2176 bp in *cbp7* null cells, respectively. The increased size (2176 bp in *cbp7* null cells) was consistent with the insertion of the *bsr* cassette into the gene. Reverse transcription (RT)-PCR using the primer set I/III and cDNA from wild-type and *cbp7* null cells confirmed that the *cbp7* gene was not transcribed in the *cbp7* null cells. No band was detected in RT-PCR experiments using cDNA from *cbp7* null cells (Fig. 3C), while a band of 510 bp was observed in RT-PCR experiments using cDNA from wild-type cells. To examine the functions of CBP7, cells overexpressing GFP-CBP7 fusion proteins (expected molecular mass of 46 kDa) were prepared, and the expression of the protein was confirmed by western blotting using anti-GFP antibodies (Fig. 3D).
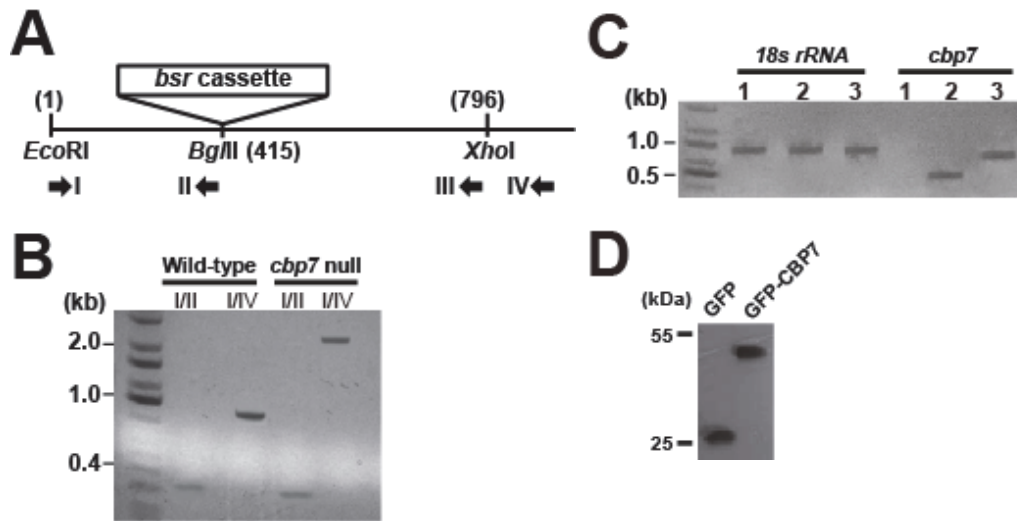
Figure 3. Confirmation of *cbp7* knockout cells and CBP7-overexpressing cells.

(A) Schematic diagram of *cbp7* knockout constructs. The *bsr* antibiotic cassette was introduced into the *cbp7* genomic DNA which was cloned into a cloning vector. Arrows and Roman numerals indicate the locations of the primers used in this study. (B) Confirmation of *cbp7* gene replacement in *cbp7* null cells. Genomic DNAs from wild-type cells and *cbp7* null cells were extracted and used in PCR with primer sets shown in panel A. (C) RT-PCR using tRNAs from wild-type and *cbp7* null cells and a primer set I/III. The universal 18s rRNA specific primers were used as an internal control. (D) Confirmation of CBP7-overexpressing cells. GFP-CBP7 was expressed in wild-type and *cbp7* null cells, and the expression of the proteins was examined by western blotting with anti-GFP antibodies (expected size of GFP-CBP7, 46 kDa).

15

III-2. CBP7 is involved in the control of cell morphology and cell adhesion

I first examined the morphology of *cbp7* null cells and GFP-CBP7 overexpressing cells (GFP-CBP7 cells) (Fig. 4A). *cbp7* null cells were smaller and more rounded than wild-type cells. In contrast, GFP-CBP7 cells were more spread and flattened than wild-type cells and *cbp7* null cells. Measurement of cell areas using the NIS-Element software showed that *cbp7* null cells were approximately half the size of wild-type cells, and GFP-CBP7 cells were 1.4-fold larger than wild-type cells (Fig. 4B). Next, I investigated cell adhesion of the cells by measuring the fraction of cells that attached to the plate during agitation. Compared to wild-type cells, cells lacking CBP7 showed decreased cell adhesion (Fig. 4C). GFP-CBP7 cells exhibited highly increased cell–substrate adhesion (Fig. 4C). The growth rates of *cbp7* null cells were similar to those of wild-type cells. However, GFP-CBP7 cells showed slower growth rates compared to both the *cbp7* null and wild-type cells (Fig. 4D). These results indicate that CBP7 is required for cell spreading and cell-substrate adhesion.

16
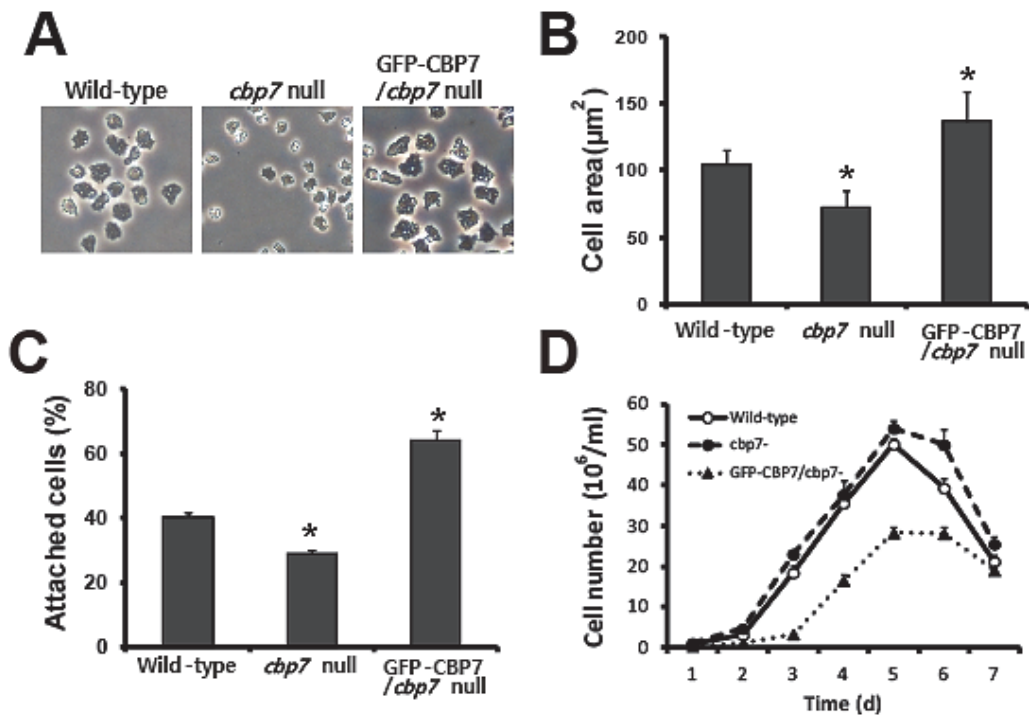
Figure 4. Cell spreading, cell adhesion, and growth rate of the cells.

(A) Morphology of wild-type cells, *cbp7* null cells, and *cbp7* null cells expressing GFP-CBP7. Exponentially growing cells were photographed. (B) Measurement of cell area. The area of the cells was measured using Image J software. The values are the means ± SD of three independent experiments (*p<0.05 compared to the control by the student's *t*-test). (C) Cell-substrate adhesion. Adhesion of the cells to the substrate was expressed as a percentage of attached cells to total cells. The values are the means ± SD of three experiments. (*p<0.05 compared to the control). (D) Growth rates of the cells. Wild-type cells, *cbp7* null cells, and *cbp7* null cells expressing GFP-CBP7 were cultured with a constant shaking of 150 rpm and counted at intervals thereafter. The means ± SD were plotted from three independent experiments.

17

III-3. Overexpression of CBP7 resulted in inhibition of development

Upon starvation, *Dictyostelium* cells release cAMP, causing surrounding cells to migrate toward the cAMP source and initiate their multicellular developmental process (Chisholm and Firtel, 2004). During development, the influx of the extracellular Ca^{2+} is stimulated by chemoattractants in *Dictyostelium* (Tanaka *et al.*, 1998). To investigate the possible roles of CBP7 in development, I examined the developmental processes of the cells (Fig. 5). Wild-type cells and *cbp7* null cells exhibited a normal developmental process, with the aggregation stage occurring within 6 h, the slug stage within 12 h, and formation of fruiting bodies within 24 h. In contrast, GFP-CBP7 cells completely lost developmental ability, even aggregation (Fig. 5A). Wild-type cells expressing GFP-CBP7 or Myc-CBP7 failed to develop, which was similar to the observation in *cbp7* null cells expressing GFP-CBP7 (Data not shown). To further investigate impairment of the aggregation stage in GFP-CBP7 cells, I examined the aggregation abilities of cells by placing them on 12-well plates containing developmental buffers instead of agar plates (Fig. 5B). In developmental buffer, wild-type cells and *cbp7* null cells started to aggregate towards an aggregation center within 6 h and formed small tight aggregates within 10 h (Fig. 5B). Contrary to wild-type cells and *cbp7* null cells, GFP-CBP7 cells did not aggregate. These results indicate that overexpression of CBP7 results in severe defects in aggregation and suggest that CBP7 is dispensable to the muticellular developmental process of *Dictyostelium* cells but plays an important inhibitory role in the initial aggregation stage of development.
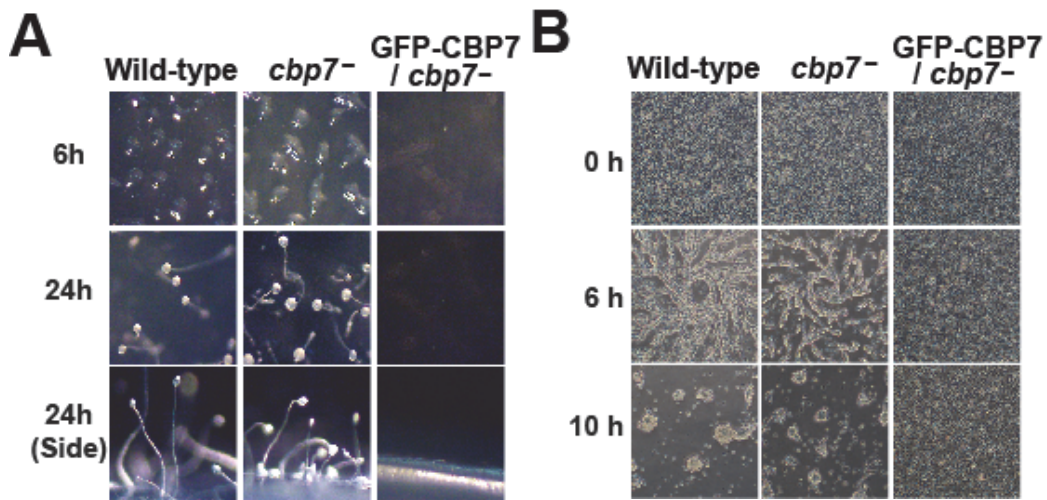
Figure 5. Development of wild-type cells, *cbp7* null cells, and GFP-CBP7 overexpressing cells.

(A) Development on non-nutrient agar plate. Exponentially growing cells were washed and plated on non-nutrient agar plates. Photographs were taken at the indicated times after plating. Representative developmental images of the cells at 6 h (aggregation stage) and at 24 h (fruiting body formation stage) are shown. Side views of fruiting bodies at 24 h are shown at the bottom row. (B) Development under submerged conditions. The cells were grown in 12-well plates. Development of the cells was induced by changing the media with non-nutrient Na/K phosphate buffer. Photographs were taken at the indicated times after induction of development.

III-4. Overexpression of CBP7 resulted in loss of directional cell migration

In contrast with wild-type and *cbp7* null cells, GFP-CBP7 cells showed no aggregation when deprived of nutrients (Fig. 5). These data suggest that GFP-CBP7 cells may have defects in chemoattractant-directed cell migration, which occurs in the initial aggregation stage of cellular development. To test this hypothesis, I performed cAMP-directed cell migration experiments using a Dunn chemotaxis chamber (Fig. 6). Aggregation-competent cells were prepared by starving the cells in Na/K phosphate buffer for 10 h (Mun et al., 2014). Wild-type cells had high moving speeds (9.1 μm/min) and directionality (0.9), which is a measure of how straight the cells move toward the chemoattractant. *cbp7* null cells moved toward increasing cAMP concentrations with similar moving speeds (10.8 μm/min) and directionality (0.8) to those of wild-type cells. In contrast, GFP-CBP7 cells had significantly decreased migration speeds (5.5 μm/ml) and directionality (0.26) compared to wild-type cells and *cbp7* null cells. GFP-CBP7 cells appeared to lose directionality and move randomly within the cAMP gradient (Fig. 6B). These results suggest that CBP7 may negatively impact cell aggregation by inhibiting cAMP-mediated directional cell migration in the aggregation stage of development.
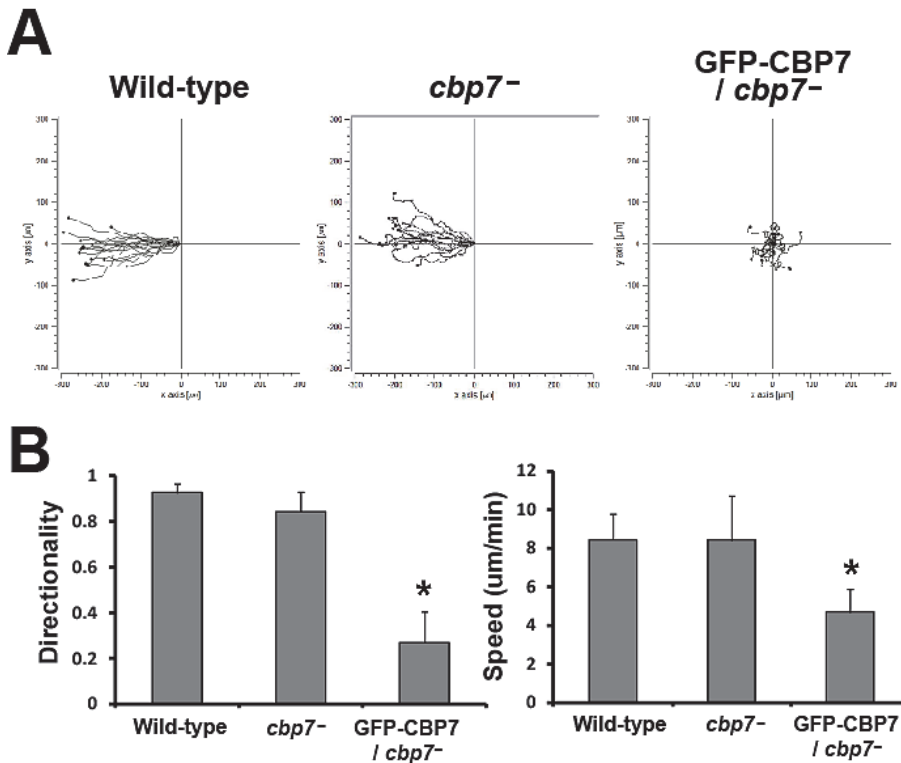
Figure 6. Chemotaxis of wild-type cells, *cbp7* null cells, and CBP7 overexpressing cells.
Aggregation-competent cells were placed in a Dunn chemotaxis chamber, and the movements of the cells up a chemoattractant, cAMP, gradient were recorded by time lapse photography for 30 min at 6 s intervals. (A) Trajectories of cells migrating toward cAMP in a Dunn chemotaxis chamber. Plots show migration paths of the cells with the start position of each cell centered at point 0. Cells migrate toward the increasing gradients of cAMP on the left. Each line represents the track of a single cell chemotaxing toward cAMP (150 μM). (B) Analysis of chemotaxing cells. The recorded images were analyzed by Image J software. Directionality is a measure of how straight the cells move. Cells moving in a straight line have a directionality of 1. Speed indicates the speed of the cells movements along the total path. The values are the means ± SD of three experiments. Statistically different from control at *$p < 0.05$ by the student's *t*-test.

21

These results related to cAMP-dependent chemotaxis were further confirmed using a cell migration assay with chimeric cells containing 95% unlabeled wild-type cells, 2.5% RFP-labeled wild-type cells, and 2.5% GFP-CBP7 expressing cells. All cells were simultaneously starved of nutrients, and the migration speeds of the labeled cells were measured during the aggregation stage of development (Fig. 7). Wild-type cells exhibited a moderate moving speed (4.53 μm/min) that was significantly higher than GFP–CBP7 cells (2.03 μm/min) during aggregation at the 6 h time point (Fig. 7B), indicating that GFP-CBP7 cells have a defect in forming aggregates by cAMP-dependent chemotaxis to the center of aggregation.

22
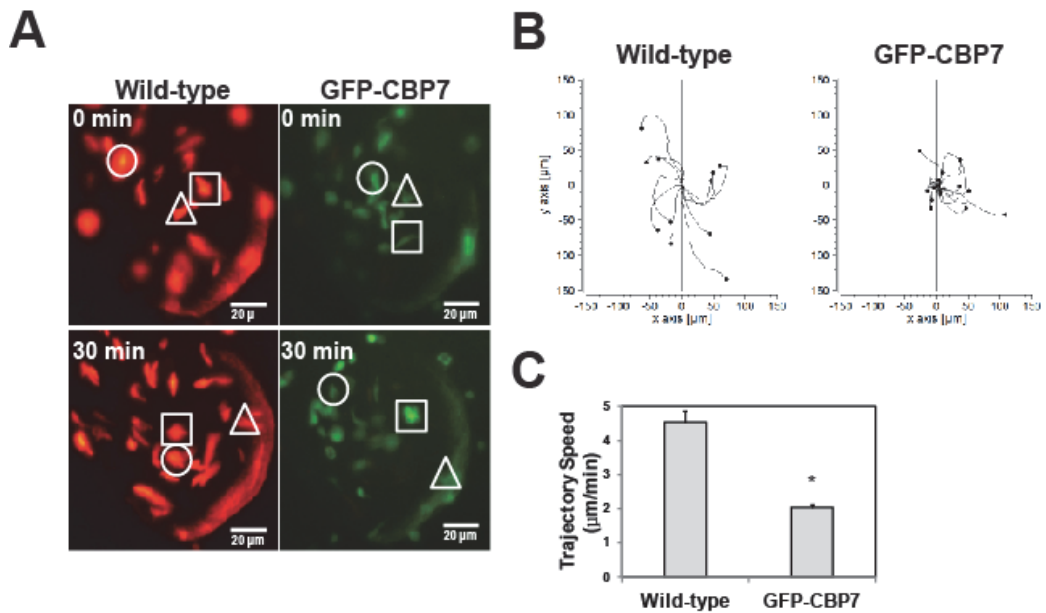
Figure 7. Analysis of cell motility during development.

For examining cell migration in the aggregation stage of development, 2.5% RFP-labeled wild-type cells and 2.5% GFP-CBP7 overexpressing cells were mixed with unlabeled 95% wild-type cells and were developed on non-nutrient agar plates. At the aggregation stage of development (6 h after development), time-lapse fluorescence images were collected to assess cell motion for 30min at 1min intervals. Two representative images at the indicated times are shown (A). Circles, rectangles, and triangles indicate representative cells analyzed and show the movements of the cells for aggregation. (B) Trajectories of cells migrating toward the aggregation center during development. Plots show migration paths of the cells with the start position of each cell centered at point 0. Each line represents the track of a single cell migrating toward the center of a circular aggregate. (C) Trajectory speeds of wild-type cells and GFP-CBP7 cells. The recorded images were analyzed by Image J software. Speed indicates the speed of the cells movements along the total path. The values are the means ± SD of three experiments. Statistically different from control at *$p<0.05$ by the student's *t*-test.

23

III-5. Overexpression of CBP7 decreased the cytosolic calcium concentration

Influx of Ca^{2+} and elevation of its level by cAMP are important in aggregation of *Dictyostelium* cells during development (Chisholm and Firtel, 2004; Siu, Sriskanthadevan et al., 2011). The calcium concentration in *Dictyostelium* rapidly increases when cell aggregation occurs (Tanaka, Itakura et al., 1998). Since CBP7 is known as a real calcium-binding protein (Sakamoto, Nishio et al., 2003), it was postulated that the cytosolic calcium concentration might be altered by the presence of CBP7. I determined the cytosolic calcium concentration in cells using the Fluo-4 calcium indicator and a fluorescence microplate reader. *cbp7* null cells had slightly higher concentrations of cytosolic calcium compared to wild-type cells. More interestingly, *cbp7* null cells expressing Myc-CBP7 exhibited significantly lower levels of free intracellular calcium than wild-type cells and *cbp7* null cells (Fig. 8). These results suggest that deregulation of free intracellular calcium levels may result in developmental defects in CBP7 overexpressing cells.

24
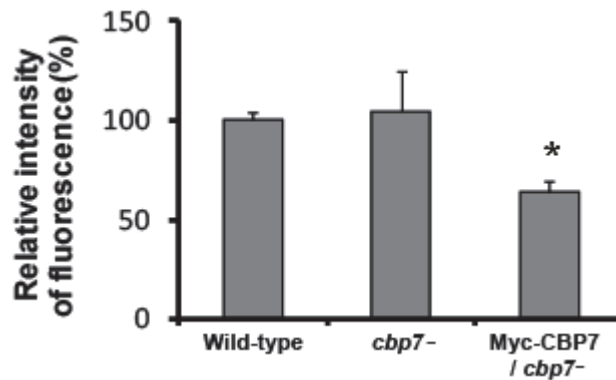
Figure 8. Measurement of the cytosolic calcium levels.

Cytosolic calcium levels in the cells were determined using the fluo-4 AM calcium indicator and a fluorescence microplate reader (exitation/emission wavelengths, 494/516 nm). The values are the means ± SD of three experiments. Statistically different from control at *p<0.05 by the student's *t*-test.

III-6. EF-hands in CBP7 are important in the process of development

Previous sequence analysis showed homology of CBP7 to other CBP proteins (Sakamoto et al., 2003). The EF-hands of CBP proteins have a helix–loop–helix structure classified into two main sub-structures, a 12-residue loop and 14-residue EF-hands. These highly conserved helix–loop–helix structures and EF-hand motifs of CBP proteins usually bind Ca^{2+} ions (Gifford et al., 2007; Trave et al., 1995). Upon binding calcium, CBP proteins, such as CBP3, undergo conformational changes resulting in the exposure of hydrophobic residues. In the presence of calcium, CBP3 interacts with other proteins; its N-terminal domain in CBP3 has a role in sensing Ca^{2+}, and the C-terminal domain undergoes a conformational change and exposes its hydrophobic region (Mishig-Ochiriin et al., 2005). CBP7 has four putative EF-hand motifs (residues D22–E33, D70–E81, D105–E116, and D140–E151). To investigate possible roles of the EF-hands of CBP7 in development, I performed point mutations into the EF-hands and prepared cells expressing point-mutated CBP7 proteins (Fig. 9). All cells expressing the point-mutated CBP7 proteins showed normal development on Na/K plates. These results indicate that all the EF-hand domains play an important role in development.
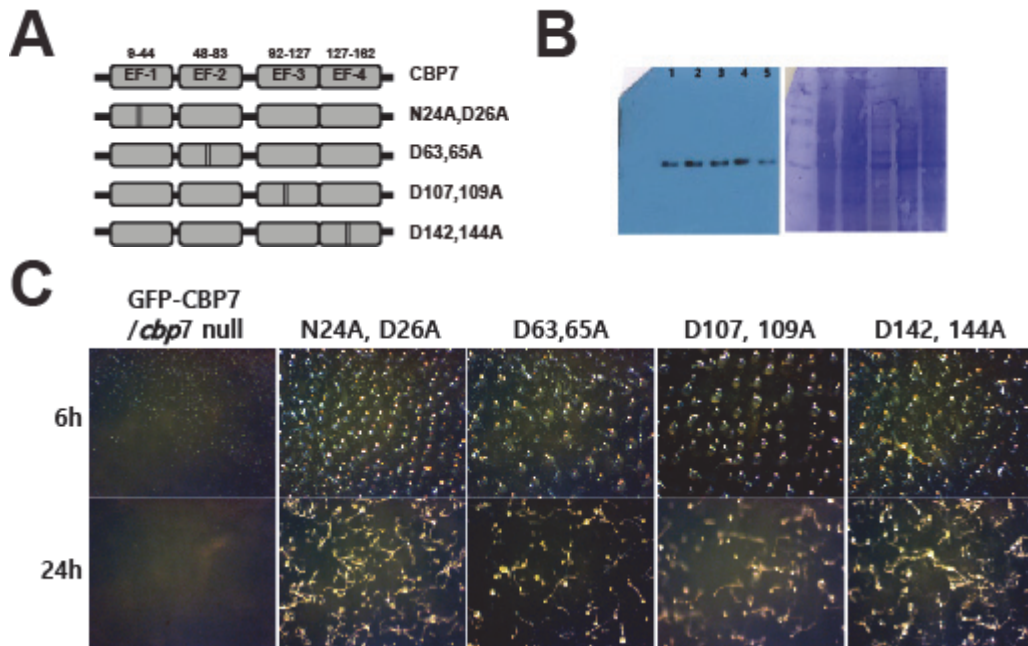
Figure 9. Development of the cells expressing point-mutated CBP7 proteins.

(A) Domain structure of the EF-hand point-mutated of CBP7. Domain structure of the EF-hand point-mutated of CBP7 and truncated CBP7 proteins. (B) Western blot analysis of EF-hand point-mutated of CBP7. 1(GFP-CBP7/*cbp7* null), 2(N24A, D26A), 3(D63, 65A), 4(D107, 109A), 5(D142, 144A). (C) Development of the cells expressing point-mutated CBP7 proteins. GFP-CBP7, CBP7[N24, D26A], CBP7[D63, 65A], CBP7[D107, 109A], and CBP7[D142, 144A]. Vegetative cells were washed and plated on non-nutrient agar plates. Photographs were taken at the indicated times after plating. Developmental images of the cells at 6 h (Wild-type aggregation stage), 12 h (Wild-type tip forming stage), and 24 h (Wild-type fruiting body stage) are shown.

27

III-7. Subcellular localization of GFP-CBP7

To examine the dynamic localization of CBP7, I prepared GFP-fusion CBP7 and expressed in the wild-type cells. The result shows that CBP7 is localized in the cytosol (Fig. 10A). To investigate the expression time of CBP7 during development, I performed RT-PCR analysis shows that CBP7 is expressed at all stages of development, with expression maximal during the late aggregation stage and then gradually decreasing until fruiting body formation (Fig. 10C).

28
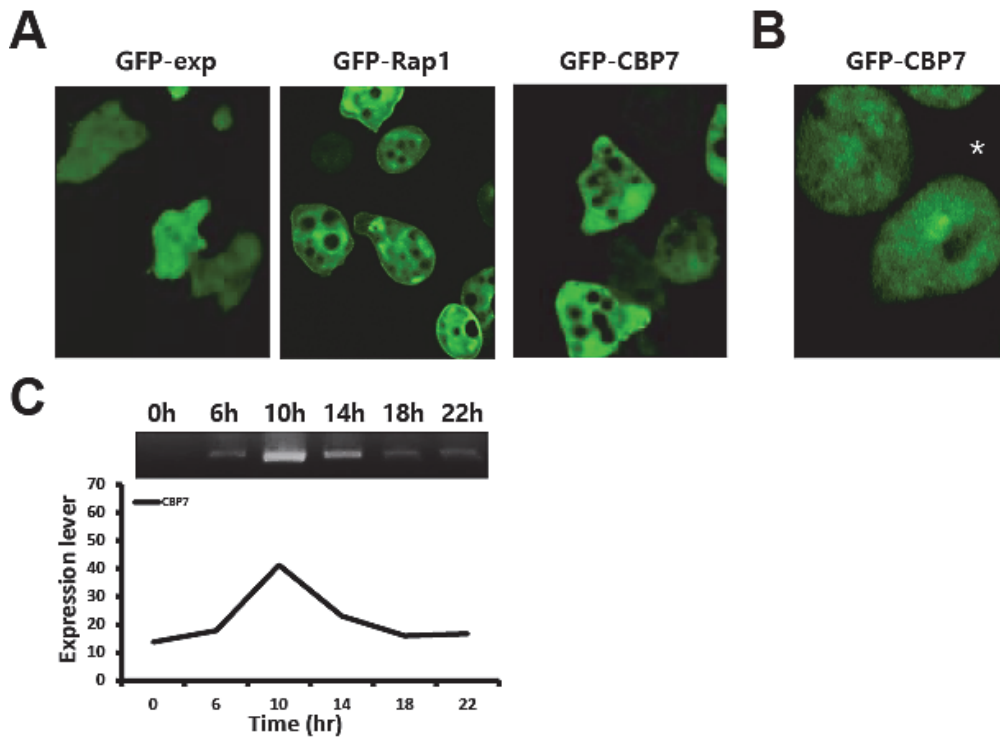
Figure 10. Localization of CBP7

(A) GFP-CBP7 in living cells. KAx3 cells expressing were placed on glass coverslips and imaged with a laser-scanning confocal microscope. (B) Localization of GFP-CBP7 during random movement. The asterisks indicate the direction of movement. (C) RT-PCR analysis of the developmental expression pattern of CBP7. I synthesized the cDNAs by reverse transcription using the RNAs isolated from developing cells at the indicated time, and amplified the 826 bp fragments at the N-described.

29

III-8. CBP7 signaling pathway

Recently, K-Ras4B, one of the mammalian Ras proteins, and the KRAS isoform were found to interact with calmodulin (Abraham et al., 2009; Nussinov et al., 2015). The Ras GTPase subfamily comprises 15 proteins in *Dictyostelium*, including 11 Ras proteins, 3 Rap proteins, and a Rheb-related protein (Kortholt and van Haastert, 2008). To determine the binding affinity to Ras proteins, I performed yeast two-hybrid experiments using CBP7 as a bait (Fig. 11A). Interestingly, the results showed that CBP7 had a strong binding affinity to RasG and a weak affinity to Rap1, if any. All other Ras proteins showed no interaction with CBP7. These results suggest that CBP7 might be a downstream effector of RasG, and provide an important clue for understanding the relationship between the Ras signaling and the calcium signaling pathways. I confirmed that CBP7 binds to RasG (Fig. 11B). To evaluate whether CBP7 was active RasG binding. The results CBP7 had binding to active RasG (Fig. 11C).
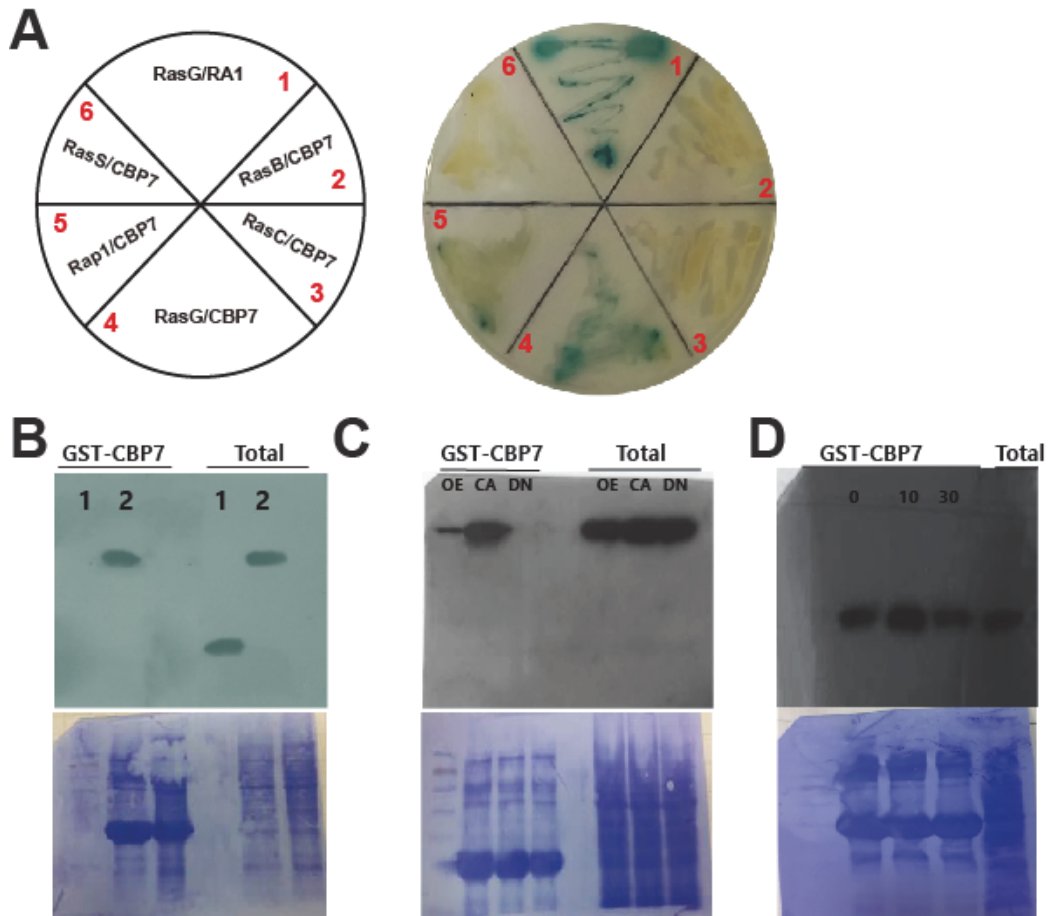
Figure 11. CBP7 binds to RasG in yeast two-hybrid analysis.

(A) Small scale yeast two-hybrid analysis of the interaction of RasG and Rap1 with CBP7. Yeast harboring both bait (pEG) and prey (pJG) plasmids grow in triple drop-out media (-Ura-His-Trp) and are positive for β-galactosidase. Interactions were evaluated by yeast growth on the plates lacking uracil, histidine and tryptophan. The numbers correspond to those in panel, 1: RasG/RA1, 2: RasB/CBP7, 3: RasC/CBP7, 4: RasG/CBP7, 5: Rap1/CBP7, 6: RasS/CBP7. (B) GFP-exp;1, and GFP-RasG;2 cells pull-down assay using a GST-CBP7. (C) The activation level of GFP-RasGOE, GFP-RasGCA, and GFP-RasGDN was assayed using a GST-CBP7 pull-down assay. (D) The activation level of RasG in response to cAMP was assayed using a GST-CBP7 pull-down assay.

31

IV. Discussion

The results demonstrate that CBP7 is required for cell spreading and cell-substrate adhesion and has a negative impact on multicellular development, possibly through inhibition of chemoattractant-mediated cell migration in the initial aggregation stage of development. *cbp7* null cells showed decreased cell size and cell-substrate adhesion. GFP-CBP7 overexpressing cells (GFP-CBP7 cells) had significantly increased cell size and cell-substrate adhesion compared to wild-type cells. Unexpectedly, overexpression of CBP7 caused severe defects in development. When deprived of nutrients, CBP7 overexpressing cells completely lost their chemotactic abilities to move toward increasing concentrations of the chemoattractant, cAMP, resulting in no cellular aggregation and formation of multicellular organisms. Cells lacking CBP7 showed normal cell migration and developed as the wild-type cells. These results suggest that CBP7 is not required for cell migration or development and that CBP7 functions as an inhibitor of cell aggregation by disrupting chemotaxis during development. Thus, during normal development of *Dictyostelium* cells, I results suggest that CBP7 should be maintained at low levels at the aggregation stage of development. In support of this conclusion, it has been reported by dictyExpress and Sakamoto et al. (2003) that CBP7 is not expressed in the vegetative state, is expressed during the slug stage of development, and then disappears at the late culmination stage (Sakamoto, Nishio et al., 2003; Rot *et al.*, 2009).

I propose one possible mechanism by which CBP7 may inhibit cell migration and development, a hypothesis that should be addressed in future studies. Low levels of intracellular calcium in CBP7 overexpressing cells resulted in the loss of directional cell migration during the aggregation stage of development. CBP7 has four highly conserved EF-hand motifs for Ca^{2+} binding, which are rich in negatively charged amino acids such as glutamic acids and aspartic acids (Gifford *et al.*, 2007) and has been demonstrated as a

32

calcium binding protein through $^{45}Ca^{2+}$-overlay experiments (Sakamoto, Nishio et al., 2003). In this study, measurement of the free intracellular calcium levels revealed that overexpression of CBP7 resulted in significantly lower levels of calcium in the cytosol and that loss of CBP7 caused slightly increased levels of intracellular calcium compared to wild-type cells. Based on previously reported data and the results presented herein, CBP7 proteins appear to directly bind to free intracellular calcium and function as a calcium buffer to lower the levels of intracellular calcium. Low level of intracellular calcium in CBP7 overexpressing cells might affect chemoattractant-directed cell migration. In agreement with our results, many studies have demonstrated that calcium ions are involved in cell migration. In *Dictyostelium* cells, Ca^{2+}-influx is stimulated by chemoattractants, which are emitted from the cells during development. Elevated intracellular Ca^{2+} level was reported to play a role in cell contraction, which is mediated by the actomyosin cytoskeleton (Malchow, Mutzel et al., 1996; Yumura, Furuya et al., 1996; Tanaka, Itakura et al., 1998). In macrophages, it was reported that Ca^{2+} influx was required for positive feedback at the leading edge of polarized cells. Inhibition of extracellular Ca^{2+} influx leads to a loss of differential leading-edge activation of PI3K and F-actin assembly (Evans and Falke, 2007).

GFP-CBP7 was found in the cytosol, and CBP7 was expressed at 6 to 10 hr of development. Functions of CBP7 EF-hand in the regulation of the developmental process were investigated in the present study. It has been reported that CBP proteins have highly conserved EF-hand domains, which are rich in negatively charged amino acids, such as glutamic and aspartic acids for Ca^{2+} binding. The EF-hand Ca^{2+}-binding motif plays an essential role in eukaryotic cellular signaling. CBP7-overexpressing cells showed developmental defects; However, point-mutated EF-hand CBP7 expressing cells, showed normal development. These data suggest that all EF-hands of CBP7 have active functions in the developmental process.

Another possibility is that CBP7 is both a calcium sensor and a downstream effecter of calcium ions, as was illustrated for CBP3 (Lee, Jeong et al., 2005; Mishig-Ochiriin, Lee et al., 2005). CBP3 has been shown to interact with the actin cytoskeleton and play important roles in cell aggregation and slug migration during development (Lee, Jeong et al., 2005). Moreover, CBP3 undergoes conformational changes upon binding to Ca^{2+}, which allows for interactions with binding partners (Mishig-Ochiriin, Lee et al., 2005). However, the roles of CBP7 seem to be opposite to those of CBP3. It was reported that cells overexpressing CBP3 showed accelerated cellular aggregation and increased numbers of small aggregates and fruiting body (Lee, Jeong et al., 2005), whereas CBP7 overexpressing cells displayed no cell aggregation and complete loss of development. A large number of proteins have been identified as CBP protein-binding partners. CBP1 and CBP3 interact with the actin cytoskeleton and CBP1 also interacts with another calcium-binding protein, CBP4a, and the actin-binding proteins, protovillin and EF-1a, in yeast two-hybrid experiments (Dharamsi, Tessarolo et al., 2000; Dorywalska, Coukell et al., 2000). Nucelomorphin, a cell cycle checkpoint protein, is a known binding protein of CBP4a (Myre and O'Day, 2004; Catalano and O'Day, 2013). I experimented progress to determine CBP7-binding proteins. According to previous studies, CaM interacts with a hypervariable region of KRAS4B but not with other Ras isoforms. KRAS4B is an oncogenic splicing isoform of KRAS, which plays an important role in cell proliferation and motility in mammalian cells (Abraham et al., 2009; Nussinov et al., 2015). There are multiple Ras proteins, of which six (RasG, RasC, RasD, RasB, RasS, and Rap1) have been characterized in *Dictyostelium* (Weeks and Spiegelman, 2003). RasG is involved in cell adhesion and development. Expression of a constitutively activated version of RasG, RasG (G12T), blocks the development (Khosla et al., 1996), and initiation of development is delayed in *ras*G-null cells (Tuxworth et al., 1997). CBP7, one of CBP proteins, plays an important role in the morphogenesis and development. In this

34

study, using a small-scale yeast two-hybrid system, I proved that CBP7 binds to active RasG. Further experiments are in progress to determine the interaction of CBP7 with RasG.

PART II. Roles of Rap Proteins in *Dictyostelium* Cell Migration and Development

I. Introduction

Chemotaxis is involved in many diverse physiological processes including the recruitment of leukocytes to the sites of infection, tracking of lymphocytes in the human body, and neuronal patterning in the developments of nervous system. Misguided cell migration results in a variety of human diseases including metastatic cancer and inflammatory diseases such as asthma and arthritis (Jin et al., 2008; Jin et al., 2009; Charest et al., 2010). Understanding of the fundamental mechanisms underlying cell migration holds the promise of effective therapeutic approaches for treating disease, cellular transplantation, and the preparation of artificial tissues (Ridley et al., 2003). A large family of small proteins, chemokines, serves as the extracellular signals, and a family of G-protein-coupled receptors (GPCRs), chemokine receptors, detects gradients of chemokines and guides cell movement *in vivo*. However, relatively little is known about the molecular mechanisms by which these receptors control chemokine-gradient sensing, the directed migration of immune and other cells (Jin et al., 2009). Filamentous actin (F-actin) is differentially polymerized at the leading edge of a cell, leading to protrusion of the membrane surface and forward movement. Assembled myosin II is preferentially found in the rear body and along the lateral sides of the cells, where it provides cortical tension and contraction of the posterior during cell movement. For efficient directional migration, cells must coordinate F-actin-mediated protrusion at the leading edge and actomyosin contraction at the cell`s posterior.

The soil amoeba *Dictyostelium discoideum*, has emerged as a powerful model system for investigating both chemotaxis and phagocytosis (Jin et al., 2009). The first step in

36

chemotaxis is the binding of chemoattractants to cell surface G-protein coupled receptors (GPCRs). In *Dictyostelium*, four cAMP receptors (cAR) have been identified. Of the identified receptors, cAR1 has a high affinity for cAMP and is essential for early development and chemotaxis. Because of their critical role in human oncogenesis Ras (Ras sarcoma) proteins have been the subject of intensive research. The *Dictyostelium* Ras GTPase subfamily comprises 19 proteins; 15 Ras, 3 Rap, and one Rheb related protein (Kortholt A and PJ. 2008).

The functions of most of these Ras proteins in development and cell migration have not been studied yet. Rap1 is the closest homologue of the small GTPase Ras and, like Ras, cycles between an inactive GDP-bound and an active GTP-bound form. Rap1 activation or deactivation is regulated by guanine nucleotide exchange factors (GEFs) and GTPase-activating proteins (GAPs), respectively (Bos and Zwartkruis 1999; Bos 2005). The Rap1 protein has an essential function in integrin mediated cell-substrate adhesion and other cell adhesion processes, as well as, phagocytosis, and cell migration in *Dictyostelium* (Jeon et al., 2007b; Kolsch et al., 2008). Recent reports have demonstrated that Rap1 is rapidly and transiently activated in response to chemoattractant stimulation with activity peaking at ~6s after chemoattractant stimulation and activated Rap1 localizing at the leading edge of chemotaxing cells (Jeon et al., 2007a). The leading-edge activation of Rap1 regulates cell adhesion and helps establish cell polarity by locally modulating Myo2 (Myosin2) assembly and disassembly through the Rap1/Phg2 signaling pathway.

To further examine the regulatory functions of Ras, I previously undertook a bioinformatics search by *Dictyostelium* genome database and identified RapB, and RapC is a Ras subfamily protein showing the high homology group with Rap1, which is a key regulator in cell adhesion and cell migration. Here, I studied the functions of RapB and RapC in diverse biological processes by examine phenotypes of several of cells expressing RapB, RapC, and mutated Ras proteins.

II. Materials and Methods

II-1. Strains, and plasmid construction

Dictyostelium wild-type KAx-3 cells, *car1/car3, gα2, and gβ* null strains were obtained from the DictyBase Stock Center. The full coding sequence of *rapB* cDNA was generated by RT-PCR and cloned into the *Eco*RI – *Xho*I site of the expression vector pEXP-4(+) containing a GFP fragment. Expression mutants, GFP-RapB [G31V] and GFP-RapB[S36N], the various mutation *rapB* sequences were amplified by PCR using site-directed mutagenesis (Table 2) and cloned into the *Eco*RI – *Xho*I site of the expression vector pEXP-4(+) containing a GFP fragment. The full coding sequence of *rapC* cDNA was generated by RT-PCR and cloned into the *Eco*RI – *Xho*I site of the expression vector pEXP-4(+) containing a GFP fragment. The *rapC* knock-out construct was made by inserting the blasticidin resistance cassette (*bsr* casstte) into *Bam*HI site created at nucleotide 535 of *rapC* gDNA and used for a gene replacement in KAx-3 parental strains. Randomly selected clones were screened for a gene disruption by PCR, which was then confirmed by RT-PCR.

II-2. DAPI staining

Exponentially growing cells were placed on the coverslip and then fixed with 3.7 % formaldehyde for 10 min. The fixed cells were washed with Na/k phosphate buffer (pH 6.1), followed by permeabilizing with 0.1 % Triton X-100, drying, and then staining with 0.5% Hoechst Dye in 1 ml of mounting solution Fluoromount-G (SouthernBiotech). Epifluorescence images of random fields of view were captured by using NIS-elements software (Nikon).

II-3. Electrotaxis assay

Dictyostelium amebae were starved in DB buffer for 1 h and seeded into an electrotaxis chamber as described previously (Zhao et al., 1996). Before electric field stimulation, two agar–salt bridges were prepared of no less than 15 cm long. The two agar–salt bridges were used to connect $AgCl_2$ electrodes in beakers with Steinberg's solution to pools of buffer at either sides of the chamber. For electric field application, the electric field strength of 20 V/cm was used. The field strength was measured at the beginning and end of the experiment (Shanley et al., 2006) .

Table 2. PCR primers sequences used for Rap study

| Gene name	primer	Sequence (5´ → 3´)
RapB mutation primer	RapB CA - F	GCAGTAATGGGCGCTGTT TCAGTTGGTAAATCAGC
	RapB CA - R	GCTGATTTACCAACTGA AACAGCGCCCATTACTGC
	RapB DN - F	CAGTTGGTAAAAATGCA CTCACTGTTCAATTCACTC
	RapB DN - R	GAGTGAATTGAACAGTG AGTGCATTTTTACCAACTG
RapC knock out primer	Ⅰ	CCCGAATTCAGTTGTTTTGGGCGCAAG
	Ⅱ	CCCGGATCCCAAAAGCTTGGGCATTTC
	Ⅲ	CCCGGATCCTATTGGTTTATTCAATTAC
	Ⅳ	CCCCTCGAGAACTATTTACATGATTAAAC
	Ⅴ	CCCGAATTCATGGATAGTTTTCAGTC
	Ⅵ	AAAATTTTTTTTATCTAGAGGATC

F – forward, R – reverse

40

III. Results

III-1. RapB

III-1-1. Identification of the gene encoding RapB

To further characterize the RapB protein, I performed computer-based analyses. *Dictyostelium* RapB (DDB_G0272857) is composed of 205 amino acids (expected molecular mass 23 kDa) and contains a RAS domain at the N-terminal region (Fig. 12A). First, I compared RapB with other RAS proteins that function is known by multiple alignment. Identical residues were highlighted in dark grey and conserved residues in light grey. Asterisks indicate the amino acid residues that are structurally or catalytically important. The RAS domain of RapB shows 86.6 % sequence identities with those of *Dictyostelium* Rap1(DDB_G0291237) RAS domain (Fig. 12B). I constructed phylogenetic trees with RAS proteins containing proteins and human RAS proteins. As shown in Figure 1C, RapB showed high homology with Rap1 (Fig. 12C). Thus, these data suggest that the RapB regulator in cell adhesion and cell migration. To examine the functions of RapB, I proposed cells overexpressing GFP-RapB, constitutively active form of RapB cells, and dominantly negative form of RapB cells fusion proteins (expected molecular mass of 50 kDa), and the expression of the protein was confirmed by western blotting using anti-GFP antibodies (Fig. 13).

41
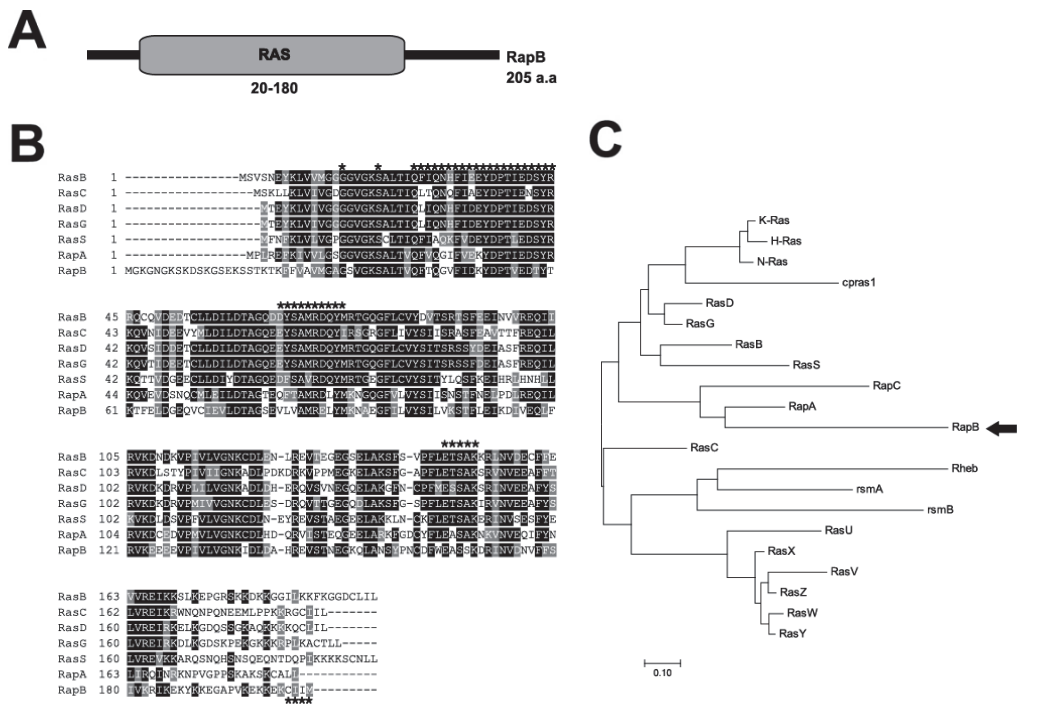
Figure 12. Domain structure and multiple alignments of RapB

(A) Domain structure of RapB. RapB contains a Ras domain in *Dictyostelium* (B) Multiple alignment of Ras domain in *Dictyostelium*: RasB, RasC, RasD, RasG, RasS, RapA. (C) Phylogenetic tree with Ras domains in *Dictyostelium* and human Ras domains. The amino acid sequences of Ras are available at dictyBase (http://www.dictybase.org. Dictyostelium discoideum Rap1 (G0291237); RapC, (G0270340); RasB, (G0292998); RasC, (G0281385); RasD (G0292996); RasG, (G0293434); RasS, (G0283537); cpras1, (G0277381); RasC, (G0281385); RheB, (G0277041); rsmA, (G0283547); rsmB, (G081253); RasU, (G0270138); RasX, (G0270124); RasV, (G0270736); RasZ, (G0270140); RasW, (G0270122); RasY, (G0270126); and RapB, (G0267456);

42

A

```
RapA    1  -----------------MPLREFKIVVLGSGGVGKSALTVQFVQGIFVEKYDPTIEDSYR
RapB    1  MGKGNGKSKDSKGSEKSSTKTKFFVAVMGAGSVGKSALTVQFTQGVFIDKYDPTVEDTYT
```

B
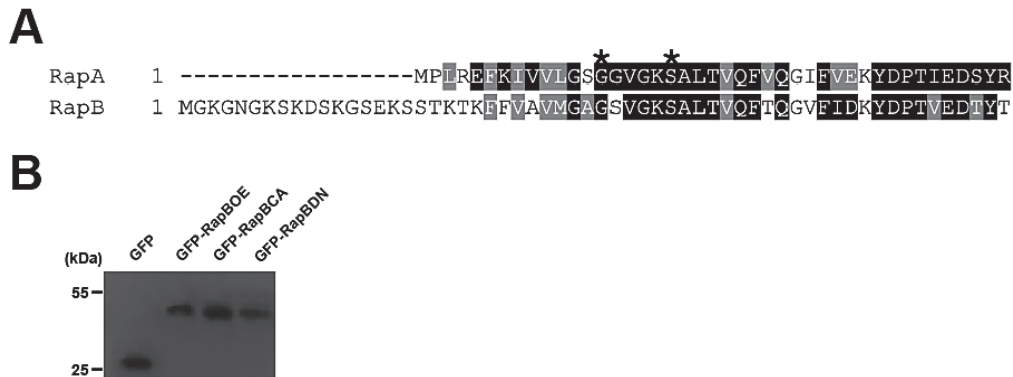
Figure 13. Constitutively active form and dominantly negative form of RapB.

(A) Schematic of mutation constructs. Confirmed point mutagenesis for GFP-RapB [G31V] and GFP-RapB[S36N] by DNA sequencing. (B) Confirmation of RapB-overexpressing, GFP-RapB [G31V] and GFP-RapB[S36N] cells. GFP-RapB was expressed in wild-type and the expression of the proteins was examined by western blotting with anti-GFP antibodies (expected size of GFP-RapB, 50 kDa).

III-1-2. RapB is involved in the control of cell morphology and cell adhesion

To investigate the function of RapB, I observed the phenotypes of wild-type and GFP-RapB expressing cells. GFP-RapB ^{G31V}cells were more spread than wild-type cells (Fig. 14A). I measured the size of the cells using NIS-element software. The mean of cell size of the GFP-RapB ^{G31V} cells was approximately 1.5-fold larger than wild-type cells (Fig. 14B). To examine the possible roles of RapB in cell adhesion, I measured the fraction of cells that Attached from bottom during agitation. GFP-RapB ^{G31V} cells showed strong attachment compared to wild-type cells. (Fig. 14C). I then investigated the effect of RapB on chemoattractant-mediated reorganization of the cytoskeleton (Fig. 14D). However, the kinetics of the response was similar to those of wild-type cells with the level of F-actin proportionally higher in GFP-RapB ^{G31V} cells. These date suggest that RapB is involved in reorganizing the cytoskeleton and cell-substrate attachment. During vegetative growth, some of the GFP-RapB ^{G31V} cells were very spread, and the size of the cells was much larger than the wild-type cells (Fig. 14D).

Examination of the number of nucleus with Hoechst dye and stained with phalloidin to detect the F-actin distribution in the cells (Fig. 15). Majority of wild-type cells contained one nucleus also RapB cells and RapB mutation cells contained one nucleus. The GFP-RapB ^{G31V} cells shoed larger F-actin than wild-type. These results suggest that RapB plays an important role in cytoskeleton and not cytokinesis.
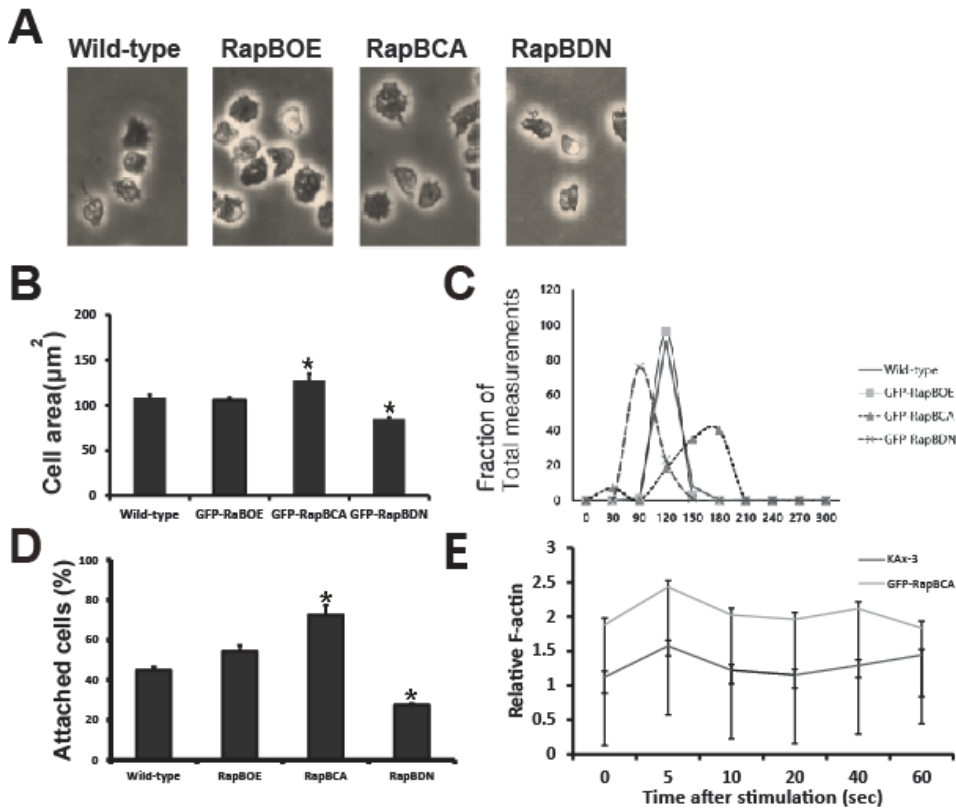
Figure 14. RapB is involved in the regulation of cell morphology and adhesion.

(A) Morphology of the vegetative cells. KAx3, GFP-RapBOE, GFP-RapB [G31V] and GFP-RapB[S36N] cells were photographed. Exponentially growing cells were photographed. (B) Analysis of the cell area. The area of the cells was measured using Image J software. The values are the means ± SD of three experiments. Statistically different from control at *p<0.05 by the student's t-test. (C) Frequency distribution of the cell area. (D) Cell-substrate adhesion. Adhesion of the cells to the substrate was expressed as a percentage of attached cells to total cells. The values are the means ± SD of three experiments. Statistically different from control at *p<0.05 by the student's t-test. (E) Kinetics of F-actin polymerization response to chemoattractant stimulation. Error bars represent ± SD of three independent experiments. (*p<0.05 compared to the control by the student's t-test).

45
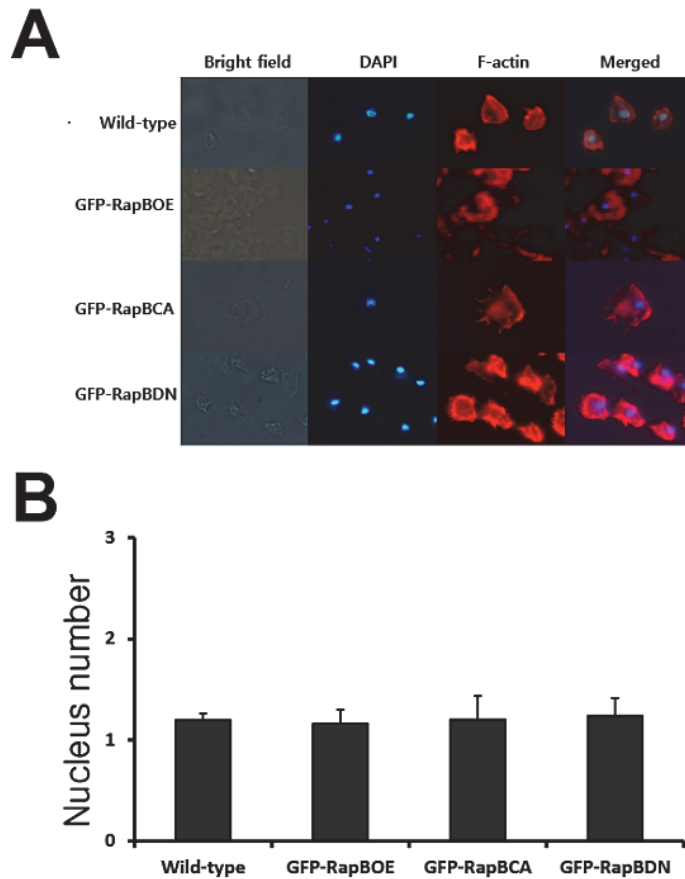
**Figure 15. The cytokinesis defect not of RapB mutation cells.**

(A) Representative DAPI and F-atin images of the cells. Corresponding phase-contrast and merged images are shown on the top and bottom panels, respectively. (B) Quantitative analysis of the number of nucleus in the cells. Mean values of the number of nuclei were graphed on the upper part. Error bars represent ± SD of three independent experiments.

46

III-1-3. RapB is required for proper cell migration and development

The chemotactic responsiveness of *Dictyostelium* cells to the chemoattractant cAMP is a developmentally regulated process in which the expression of both the major cAMP chemoattractant receptor (cAR1) and the coupled Gα subunit (Gα2) is very low during vegetative growth and is induced to high levels during the early stages of development before aggregation. Wild type cells are fully competent to respond to cAMP, maximally induce known signaling pathways required for chemotaxis. The cells at early stage of development become highly polarized when placed in a chemoattractant gradient. To examine the possible role of RapB in cell movement, I examined the ability of RapB expressing cells to polarize and chemotax up a cAMP chemoattractant gradient by using Image J software and NIS-element software. When the cells are exposed to the chemoattraet gradients, the wild-type cells became highly elongated and polarized and moved fast with average speed of approximately 15 μm/min. GFP-RapB^{G31V} cells were polarized, but the moving speed was slightly lower than that of wild-type cells (Fig. 16). In addition, the directionality, which is a measure of how straight the cells move, of GFP-RapB^{G31V} cells were lower than that of wild-type cells. These data suggest that RapB is required for proper cell migration and possibly in involved in directional sensing during chemotaxis.
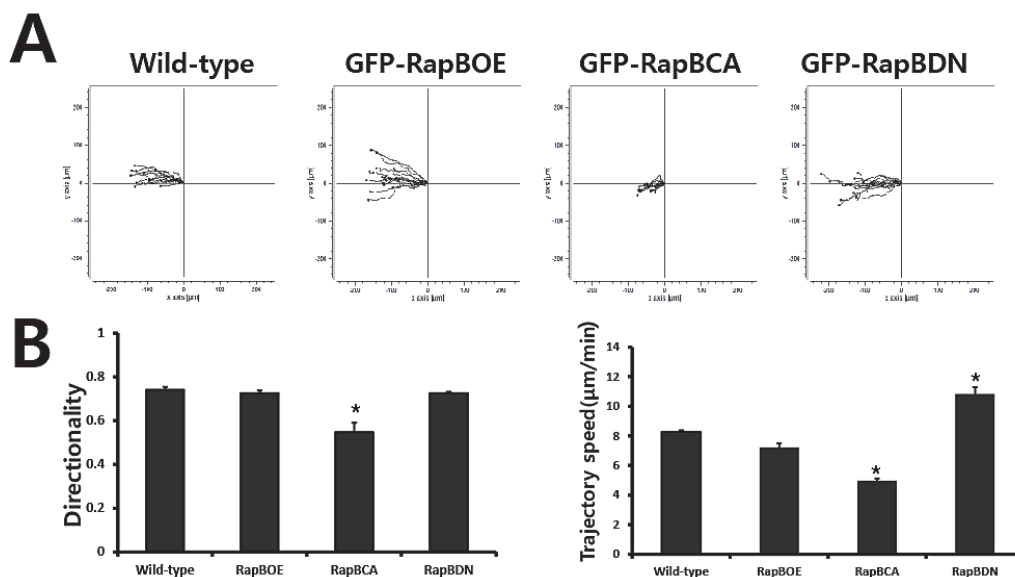
Figure 16. Chemotaxis of wild-type cells, GFP- RapB, GFP- GFP-RapB ^{G31V} and GFP-RapB^{S36N} cells.

Aggregation-competent cells were placed in a Dunn chemotaxis chamber, and the movements of the cells up a chemoattractant, cAMP, gradient were recorded by time lapse photography for 30 min at 6 s intervals. (A) Trajectories of cells migrating toward cAMP in a Dunn chemotaxis chamber. Plots show migration paths of the cells with the start position of each cell centered at point 0. Cells migrate toward the increasing gradients of cAMP on the left. Each line represents the track of a single cell chemotaxing toward cAMP (150 μM). (B) Analysis of chemotaxing cells. The recorded images were analyzed by Image J software. Directionality is a measure of how straight the cells move. Cells moving in a straight line have a directionality of 1. Speed indicates the speed of the cells movements along the total path. Error bars represent ± SD of three independent experiments. Statistically different from control at *$p < 0.05$ by the student's *t*-test.

During development, *Dictyostelim* cells release chemoattractant cAMP, insitiating surrounding cells migrate, and the formation of a multicellular fruiting body (Chisholm RL 2004). To examine the possible in vivo roles of RapB in cell motilit, and development, I performed development assay.   As shown in Figure 6A, GFP-RapB ^{G31V} cells aggregated slightly delayed to form mound at ~8h with timing and morphology differently to those of wild-type cells. Also, the formation of fruiting body was slightly delayed in GFP-RapB ^{G31V} cells compared to wild type cells (Fig. 17A). The growth rates of wild-type, GFP-RapBOE, GFP-RapB ^{G31V} and GFP-RapB ^{S36N} strains were determined at the indicated times and the plotted values are the means of duplicate hemocytometer counts. The growth of the GFP-RapB ^{G31V} strain was delayed from that of wild-type cells in suspension (Fig. 17B). These results indicate RapB is required for proper devlopment.
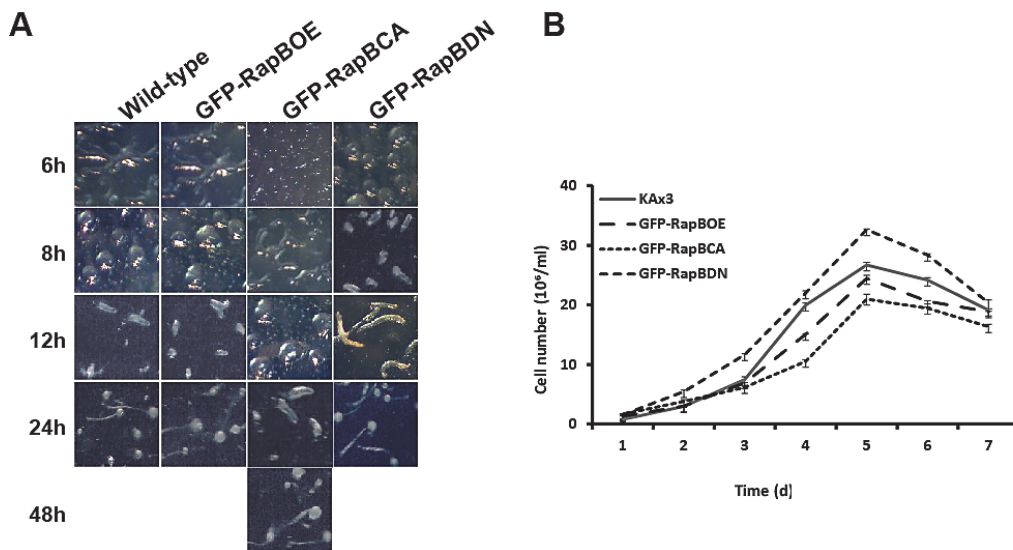
Figure 17. Development of wild-type cells, GFP-RapBOE, GFP-RapB ^{G31V} and GFP-RapB^{S36N} cells.

(A) Development on non-nutrient agar plate. Exponentially growing cells were washed and plated on non-nutrient agar plates. Photographs were taken at the indicated times after plating. Representative developmental images of the cells at 6 h (aggregation stage) and at 24 h (fruiting body formation stage) are shown. (B) Growth rates of the cells. Wild-type cells, GFP-RapBOE, GFP-RapB ^{G31V} and GFP-RapB^{S36N} cells were cultured with a constant shaking of 150 rpm and counted at intervals thereafter. The means ± SD were plotted from three independent experiments.

50

III-1-4. RapB localization

I investigated RapB localization using GFP-RapB. GFP-RapB localized predominantly to the intracellular membranes, including the ER and endosomal membranes. In addition, a portion of GFP-RapB was present on the plasma membrane. GFP-RapB showed a similar localization to Rap1 in chemotaxing cells and is absent from the domain immediately posterior to the leading edge, presumably because the endosomal membrane fraction is excluded by the pseudopodial F-actin cortex (Fig. 18A and 18B). To investigate the expression time of RapB during development, I performed RT-PCR analysis shows that RapB is expressed at all stages of development, with expression maximal during the early and end stage of development (0 to 6 and 18 to 22hr) (Fig. 18C).
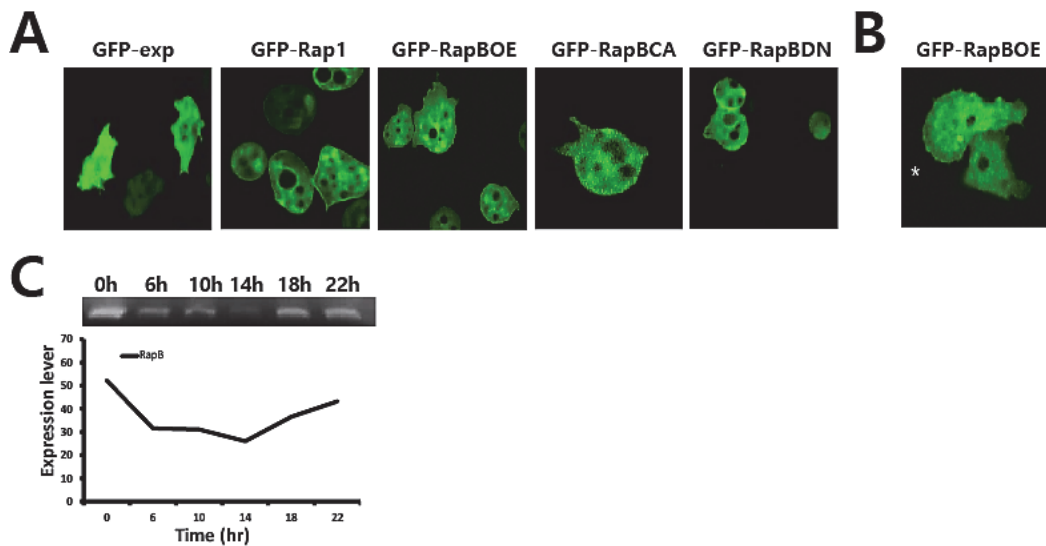
Figure 18. Localization of GFP-RapB

(A) Localization of GFP-exp, GFP-Rap1, GFP-RapBOE, GFP-RapB ^{G31V}, and GFP-RapB^{S36N} in living cells. (B) Localization of GFP-RapBOE during random movement. The asterisks indicate the direction of movement. (C) RT-PCR analysis of the developmental expression pattern of RapB. I synethesized the cDNAs by reverse transcription using the RNAs isolated from developing cells at the indicated time, and amplified the 615 bp fragments at the N-described.

III-2. RapC

III-2-1. Identification of the gene encoding RapC

To further characterize the RapC protein, I performed computer-based analyses. *Dictyostelium* RapC (DDB_G0270340) is composed of 278 amino acids (expected molecular mass 30 kDa) and contains a RAS domain at the N-terminal region (Fig. 19A). First, I compared RapC with other RAS proteins by multiple alignments. Identical residues were highlighted in dark grey and conserved residues in light grey. Asterisks indicate the amino acid residues that are structurally or catalytically important. The RAS domain of RapC shows 50.9 % sequence identities with those of *Dictyostelium* Rap1 (DDB_G0291237) RAS domain (Fig. 20). I constructed phylogenetic trees with RAS proteins containing human RAS proteins. RapC shows high homology with Rap1 (Fig. 19B). Thus, these data suggest that the RapC regulator in cell adhesion and cell migration.

53
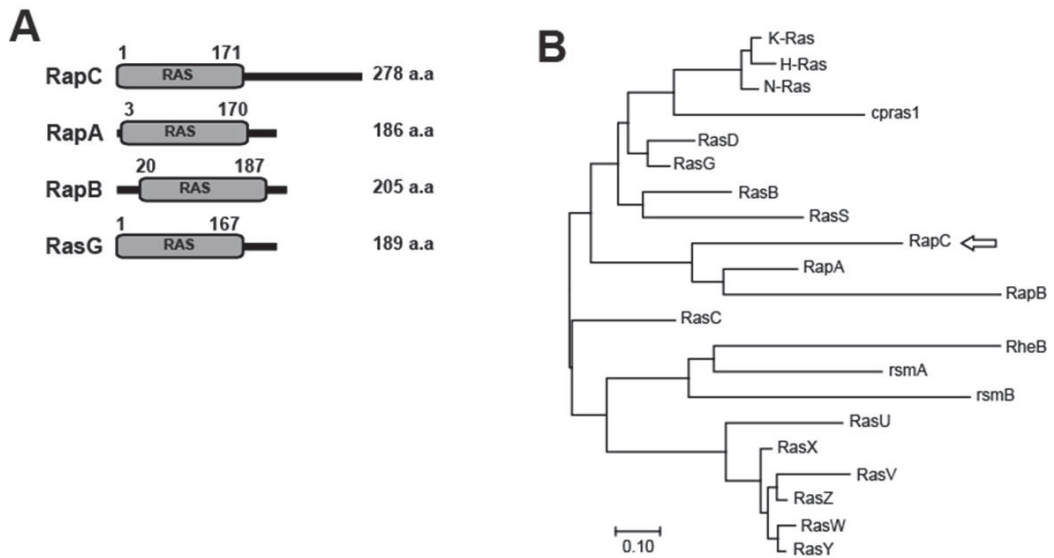
Figure 19. Domain structure and phylogenetic tree of RapC in *Dictyostelium.*

(A) Domain structure of the *Dictyostelium* RapC showing RapC domain in the N-terminus.

(B) Phylogenetic tree with Ras domains in *Dictyostelium* and human Ras domains. Rap1
(G0291237); RapB, (G0267456); RasB, (G0292998); RasC, (G0281385); RasD
(G0292996); RasG, (G0293434); RasS, (G0283537); cpras1, (G0277381); RasC,
(G0281385); RheB, (G0277041); rsmA, (G0283547); rsmB, (G081253); RasU, (G0270138);
RasX, (G0270124); RasV, (G0270736); RasZ, (G0270140); RasW, (G0270122); RasY,
(G0270126); and RapC, (G0270340); These sequences are available at www.dictybase.org
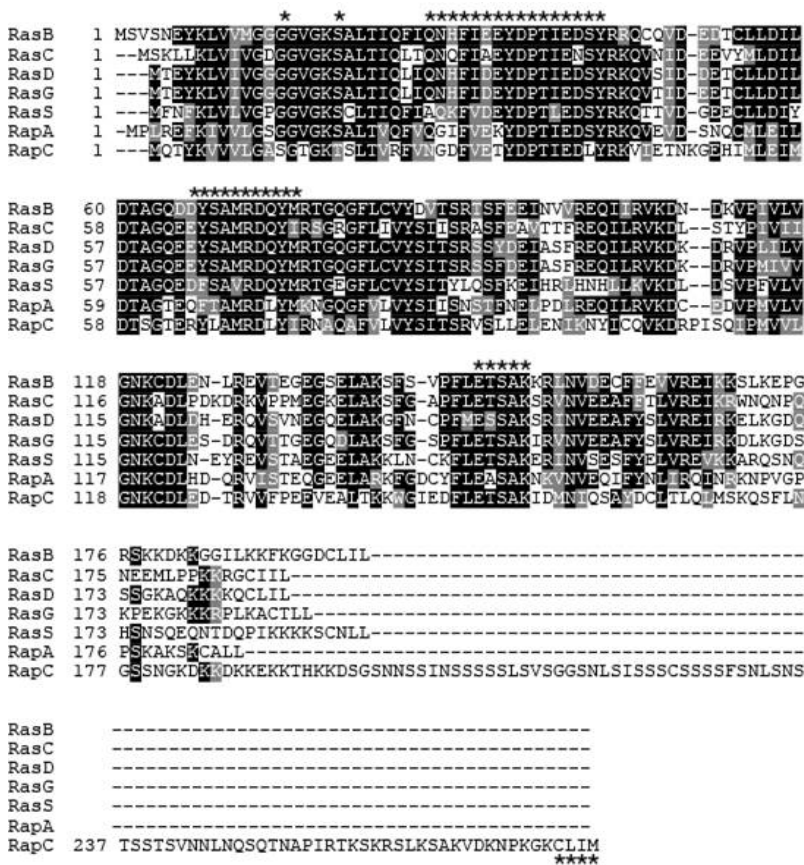
54

Figure 20. Multiple alignment of RAS protins.

The amino acid sequence of a RAS domain of RapC was compared with other RAS proteins. RapA (G0291237); RasB, (G0292998); RasC, (G0281385); RasD (G0292996); RasG, (G0293434); RasS, (G0283537); and RapC, (G0270340); These sequences are available at www.dictybase.org.

55

To investigate the functions of RapC, I prepared *rapC* knock-out strains by homologous recombination with the *rapC* knock-out DNA construct containing a blasticidin resistance (*bsr*) antibiotic cassette into the *rapC* genomic DNA of KAx-3 parental strains (Fig. 21A). *rapC* knock-out cells were confirmed by polymerase chain reactions (PCR) (Fig. 21B). PCR with a set of primers, I/III, I/Ⅳ and I/V, produced bands of 535, no band, and 1151 bp in wild-type cells and bands of 535, 535, and 2501 bp in *rapC* null cells, respectively. The increased size (2500 bp in *rapC* null cells) was consistent with the insertion of the *bsr* cassette into the gene. Reverse transcription (RT)-PCR using the primer set Ⅳ/V, and I/V cDNA from wild-type and *rapC* null cells confirmed that the *rapC* gene was not transcribed in the *rapC* null cells. No band was detected in RT-PCR experiments using cDNA from *rapC* null cells (Fig. 21C), while a band of 615 bp was observed in RT-PCR experiments using cDNA from wild-type cells. To examine the functions of CBP7, cells overexpressing GFP-RapC fusion proteins (expected molecular mass of 57 kDa) were prepared, and the expression of the protein was confirmed by western blotting using anti-GFP antibodies (Fig. 21D).

56
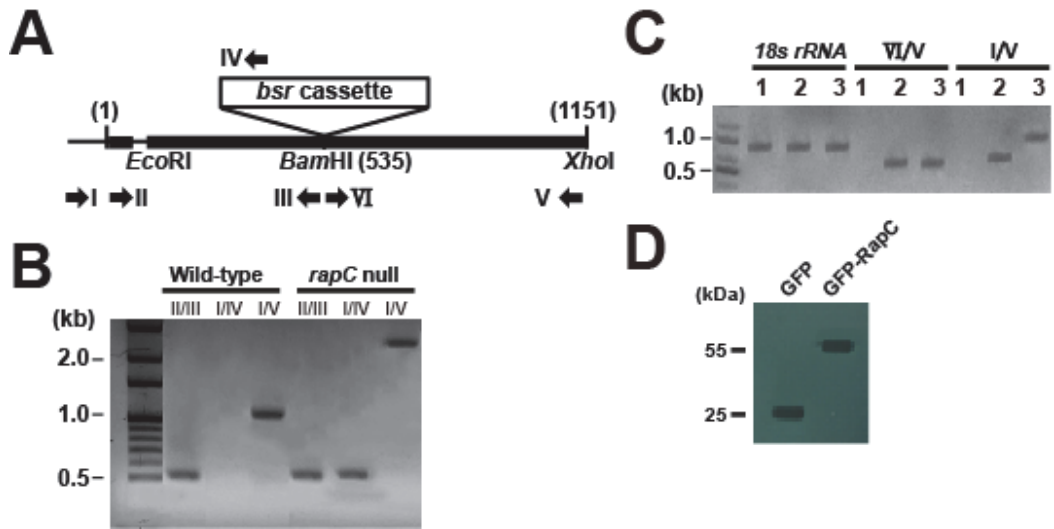
Figure 21. Confirmation of a *rapC* knockout cells and RapC-overexpressing cells.

(A) Knock-out construct diagram. The *bsr* antibiotic cassette was introduced into the *rapC* complementary DNA which was cloned into a cloning vector. Arrows and Roman numerals indicate the locations of the primers used in this study. (B) Validation of *rapC* null cells by PCR analysis. Primers are denoted by Roman numerals and arrows. (C) The expression of *rapC* in *rapC* null cells was confirmed by RT-PCR. The 18S ribosomal RNA specific primers were used as an internal control. (D) Confirmation of RapC-overexpressing cells. GFP-CBP7 was expressed in wild-type and *rapC* null cells, and the expression of the proteins was examined by western blotting with anti-GFP antibodies (expected size of GFP-RapC, 57 kDa).

57

III-2-2. RapC is involved in the regulation of morphology and cytokinesis

To investigate the function of RapC, I observed the phenotypes of wild-type, *rapC* null cells, and RapC overexpressing cells. Compared to wild-type cells, some of *rapC* null cells were more flat and spread out, and highly multinucleated (Fig. 22A). I measured the size of the cells using NIS-element software. The mean cell size of the rapGAP9 null cells was approximately 3-fold larger than wild-type cells (Fig. 22B). The morphological phenotype of *rapC* null cells was complemented by expressing RapC, suggesting a function of RapC's on the cell shape formation. To examine the possible roles of RapC in cell adhesion, I measured the fraction of cells that detach from a membrane during agitation. *rapC* null cells showed strong attachment compared to wild-type cells and this was partially complemented in GFP-RapC expressing cells (Fig. 22C). The growth rate of the *rapC* null strain was indistinguishable from wild-type cells in suspension (Fig. 22D). These data suggest that RapC is involved in reorganizing the morphology and cell–substrate attachment.

Next, examination of the number of nucleus showed that *rapC* null cells have a cytokinesis defect. Majority of wild-type cells contained one nucleus, whereas most of *rapC* null cells had two nuclei and some of the cells over eight nuclei (Fig. 23). The introduction of RapC into *rapC* null cells rescued the cytokinesis defect of the null cells and the *rapC* null cells expressing RapC showed normal number of nucleus. These results suggest that RapC plays an important role in morphogenesis and cytokinesis.
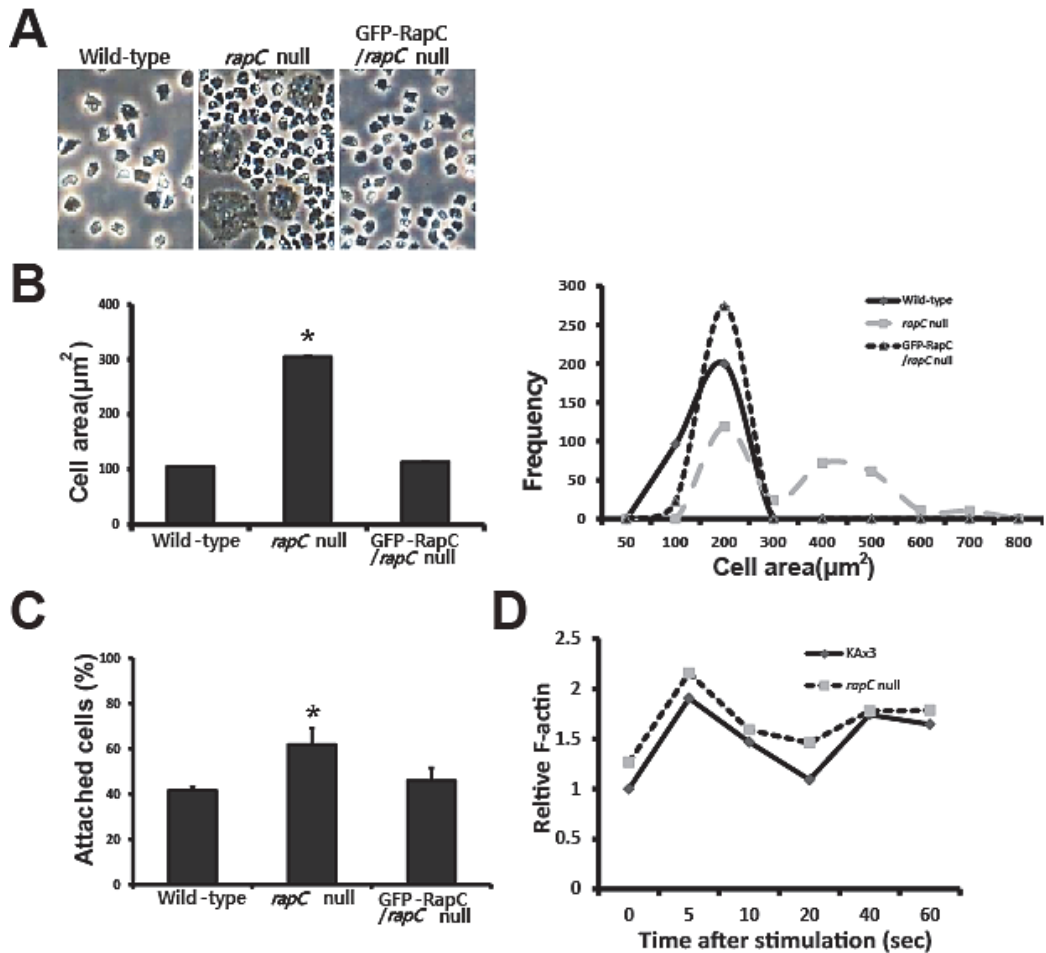
Figure 22. Phenotypes of *rapC* null and RapC overexpressing cells.

(A) Morphology of the vegetative cells. Wild-type cells, *rapC* null cells, and GFP-RapC expressing cells were photographed. (B) Measurement of cell areas of cell using NIS-element software. The values are the means ± SD of three independent experiment. (*$p<0.05$ compared to the control by the student's *t*-test). Frequency of the cell area is shown. (C) Cell-substrate adhesion assays. Adhesion of the cells to the substrate was expressed as a percentage of attached cells to total cells. The values are the means ± SD of three independent experiment. (*$p<0.05$ compared to the control). (D) Kinetics of F-actin polymerization response to chemoattractant stimulation.
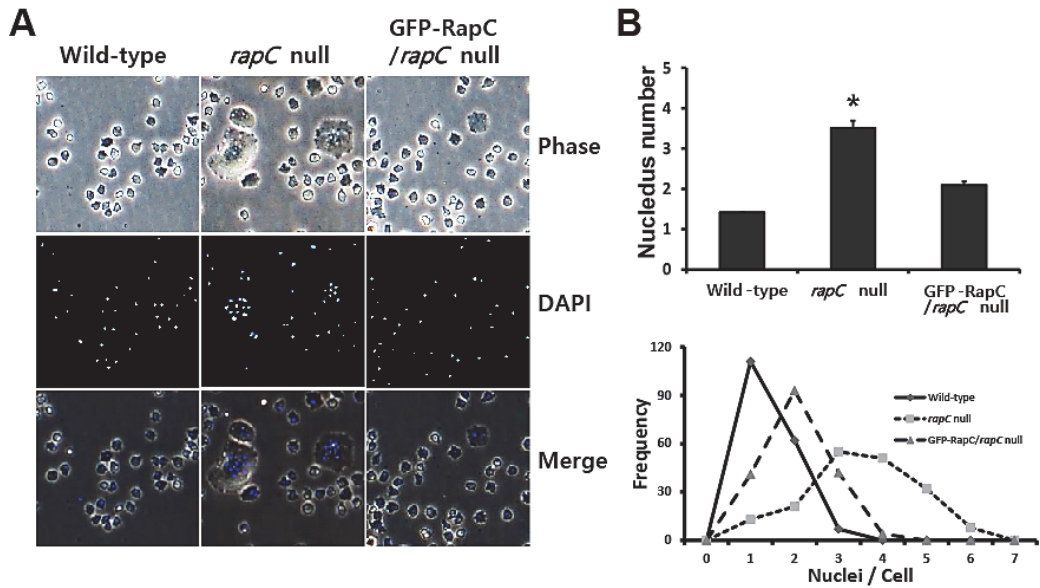
Figure 23. The cytokinesis defect of *rapC* null cells.

(A) Morphology of the cells. Vegetatively grow wild-type, *rapC* null cells, and *rapC* null cells expressing GFP-RapC. (B) Representative DAPI images of the cells. Correseponding phase-contrast and merged images are shown on the top and bottom panels, respectively. Quantitative of the number of nucleus in the cells. Mean values of the number of nuclei were graphed on the upper pot and the frequency distribution was compared on the lower pot. Error bars represent ± SD of three independent experiment. Statistically different from control at *p<0.05 by the student's t-test.

III-2-3. RapC required for proper cell migration and development

The previous sequence analysis showed the homology of RapC with Rap1, which are required for proper cell migration. In addition, the phenotypes of *rapC* null cells are very similar to those of cells expressing constitutively active Rap1. These data raised a possibility of involvement of RapC in cell migration and developmental process in *Dictyostelium*. Therefore, I examined development in *Dictyostelium*, cells release cAMP, causing surrounding cells to migrate and initiate the formation of a multicellular fruiting body. To examine the possible roles of RapC in development, I performed a developmental assay. wild-type cells aggregated normally to form a mound at 8 h. However, *rapC* null cells aggregated slightly delayed than wild-type, and *rapC* null cells had multiple fruiting bodies. Expression of GFP-RapC in *rapC* null cells complemented the developmental phenotypes of *rapC* null cells, with developmental timing and morphologies similar to the parental wild-type strain. (Fig. 24). These results indicate RapC is required for proper development.

Next, the ability of *rapC* null cells to polarize and chemotax up a cAMP chemoattractant gradient using Dunn chemotaxis chamber. *rapC* null cells moved toward a higher concentration of cAMP but the moving speed was slightly lower than that of wild-type cells (Fig. 25). In addition, the directionality, which is a measure of how straight the cells move, *rapC* null cells was lower than wild-type cells. These data suggest that RapC plays for positive cell migration during chemotaxis. And, it is known that electrotaxis is required for migration in fruiting bodies of development in *Dictyostelium.* To investigate the possible roles of RapC in electrotaxis, I compared the directedness and velocity of wild-type cells, *rapC* null, and GFP–RapC/*rapC* null cells. The *rapC* null cells directionality and moving speed in electrotaxis were delayed than wild-type (Fig. 26). These results indicate that RapC plays for positive cell migration during electrotaxis in *Dictyostelium*.
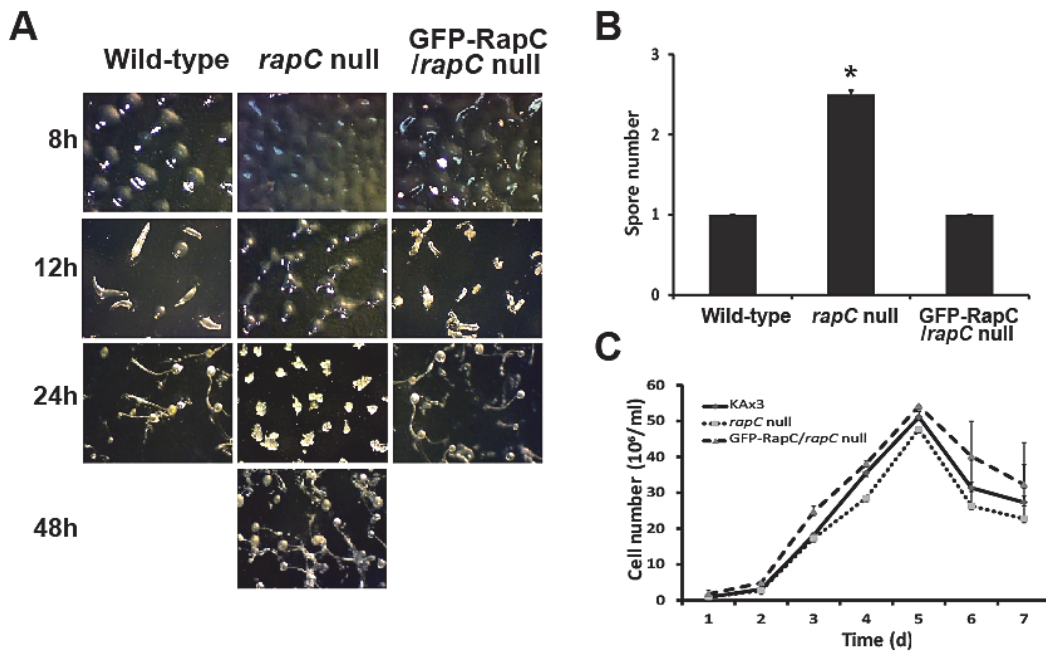
Figure 24. Development of wild-type cells, *rapC* null cells and the cells overexpressing RapC.

(A) Development on non-nutrient agar plate. Exponentially growing cells were washed and plated on non-nutrient agar plates. Photographs were taken at the indicated times after plating. Representative developmental images of the cells at 6 h (aggregation stage) and at 24 h (fruiting body formation stage) are shown. Development of *rapC* null cells was delayed, and multiple fruiting bodies. (B) Analysis of the spore number at 24 hr. *rapC* null cells has and multiple fruiting bodies. (C) Growth rates of the cells. Wild-type cells *rapC* null, and GFP-RapC cells were cultured with a constant shaking of 150 rpm and counted at intervals thereafter. The means ± SD were plotted from three independent experiments.

62
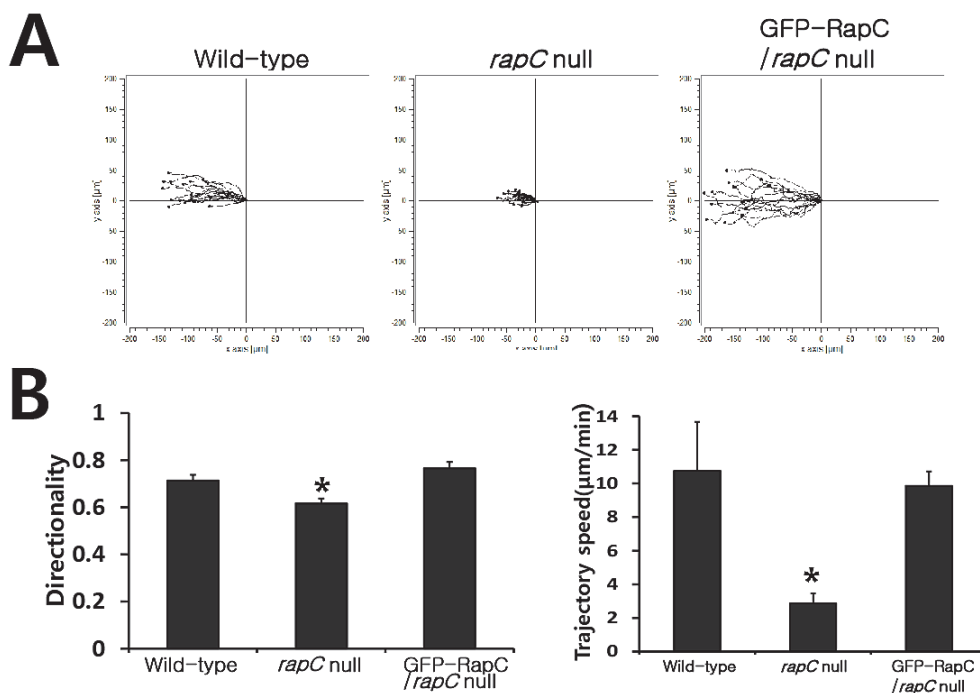
Figure 25. Analysis of chemotaxis using Image J software and NIS-element software.

Aggregation competent cells from wild-type or *rapC* null cells were placed in a Dunn chemotaxis chamber, and the movements of the cells up a chemoattractant (cAMP) gradient were recorded by time lapse photography for 30 min at 6 sec intervals. (A) Trajectories of cells migrating toward cAMP in Dunn chemotaxis chamber. Trajectories were tracked with Image J software. Each line represents the track of a single cell chemotaxing toward cAMP (150 μM). (B) Analysis of chemotaxing cells. The recorded images were analyzed by NIS-element software. Directionality is a measure of how straight the cells move. Cells moving in a straight line have a directionality of 1. It is calculated as the distance moved over the linear distance between the start and the finish. Wild-type cells show a significantly higher directional movement towards an apical region of the organism than *rapC* null cells. Speed indicates the speed of the cell's movement along the total path. Error bars represent ± SD of three independent experiment. (*$p < 0.05$ compared to the control by the student's *t*-test).

63
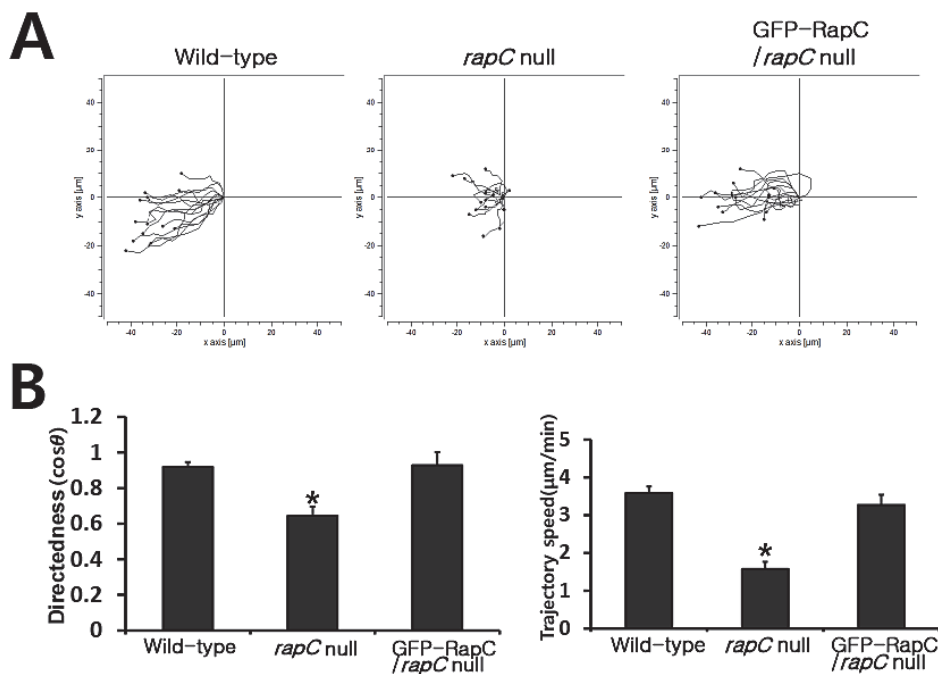
Figure 26. Analysis of cell motility in electrotaxis

4 hours starvation competent cells from wild-type, *rapC* null cells, and GFP-RapC/*rapC* null cells were placed in a electrotaxis chamber, (A) and the movements of the cells up a direction of electric field were recorded by time lapse photography for 60 min at 1min intervals. (B) Velocity speeds increased significantly in both types of cells following field stimulation. Wild-type and GFP-RapC/*rapC* null cells migrate towards the cathode with similar direction of cell migration. The graphs show migration of cells in an electric field of 20 V/cm and take, average of 63-68 cells. The instantaneous velocity is being calculated for a particular cell and it is the time interval between frames. Directedness was assessed as cosine θ, a cell moving directly to the cathode would have a directedness of 1, whereas a cell moving directly to the anode would have a direction of migration of −1. Experiments were performed at least three times. Error bars represent ± SD of three independent experiment. (*$p<0.05$ compared to the control by the student's *t*-test).

64

### III-2-5. RapC localization and signaling pathway

To examine the dynamic localization of RapC, I prepared GFP-fusion RapC and expressed in the wild-type cells. The result shows that RapC is localized predominantly to the intracellular membranes, including the ER and endosomal membranes (Fig. 27A). In addition, a portion of GFP-RapC was present on the plasma membrane. GFP-RapC showed similar localization to Rap1 and RapB in chemotaxing cells and is absent from the domain immediately posterior to the leading edge, presumably because the endosomal membrane fraction is excluded by the pseudopodial F-actin cortex (Fig. 27B).

To investigate the expression time of RapC during development, I performed RT-PCR analysis shows that RapC is expressed at all stages of development, with expression maximal during the late aggregation stage and maintain until fruiting body formation (Fig. 27C). To determine the mechanism for the upstream signal of RapC, I employed a pull-down assay using the RBD of RalGDS and anti-GFP antibodies. Interestingly, wild-type cells showed a rapid activation of RapC with a peak at 5 to 10 s in response to chemoattractant stimulation and then deactivation to the basal level within 40s. In contrast, the mutant strains, *car1/car3* null cells, gα null cells and gβ null cells exhibited a low basal level of RapC-GTP before stimulation, compared to wild-type cells, and the level did not change upon chemoattractant stimulation (Fig. 27D).

65
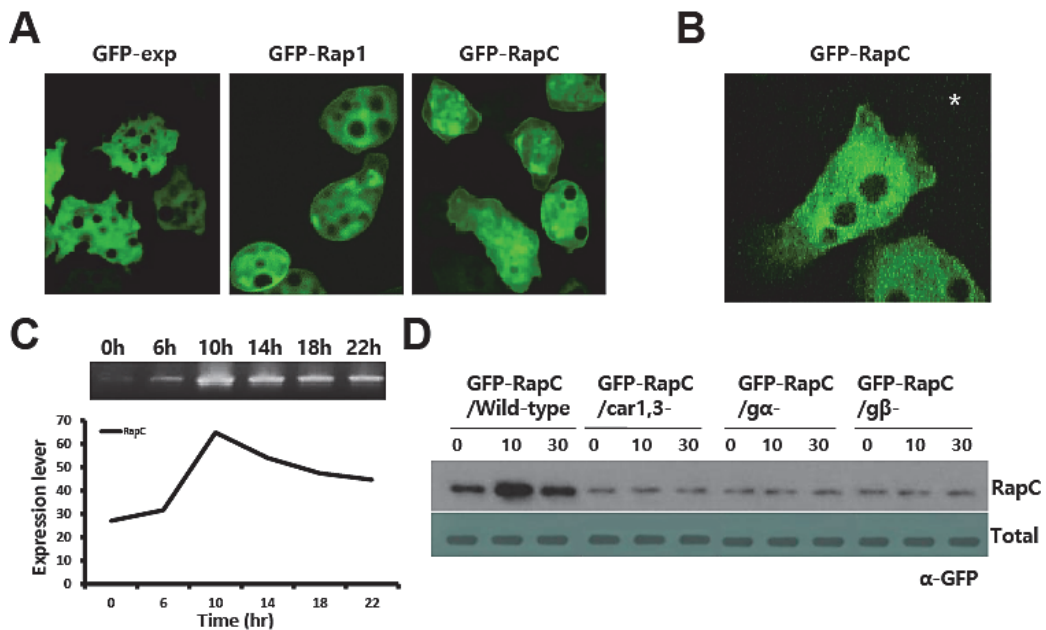
Figure 27. Localization of GFP-RapC and chemoattractant-mediated RapC activation in cells lacking GPCR/G proteins.

(A) Localization of GFP-exp, GFP-Rap1, and GFP-RapC in living cells. (B) Localization of GFP-RapC during random movement. The asterisks indicate the direction of movement. (C) RT-PCR analysis of the developmental expression pattern of RapC. I synethesized the cDNAs by reverse transcription using the RNAs isolated from developing cells at the indicated time, and amplified the 1151 bp fragments at the N-described. (D) Aggregation-competent cells were treated with 15 μM cAMP for the indicated times. The activation level of RpaC-GTP-binding domain proteins and an anti-GFP antibody. Total means the same volume of each lysate.

IV. Discussion

The small GTPase Rap1 is involved in the control of diverse cellular processes, including integrin-mediated cell adhesion, cadherin-based cell-cell adhesions, cell polarity formation, and cell migration. Identified RapB and RapC are Ras subfamily proteins showing the high homology with Rap1, which is a key regulator in cell adhesion and cell migration (Jeon et al., 2007a).

I results demonstrate that RapB is positive plays for cell spreading and cell-substrate adhesion and has a negative impact on development. Dominantly negative form of GFP-RapB cells (GFP-RapB^{S36N} cells) showed decreased cell size and cell-substrate adhesion. Constitutively active form of GFP-RapB cells (GFP-RapB^{G31V} cells) had increased cell size and cell-substrate adhesion compared to wild-type cells. When deprived of nutrients, GFP-RapB^{S36N} cells showed elevate chemotactic abilities to move toward increasing concentrations of the chemoattractant due to weak adhesion, resulting in fast cellular aggregation and early formation of multicellular organisms than wild-type cells. In contrast, GFP-RapB^{G31V} cells showed slow cell migration and developed than wild-type cells. These results suggest that RapB required for positive cell migration and development.

GFP-fusion RapB cells appears to localize to the plasma membrane. In chemotaxing cells, GFP-RapB was observed at the immediately posterior to the leading edge. I results suggest that active-RapB is absent from the domain immediately posterior to the leading edge, presumably because the endosomal membrane fraction is excluded by the pseudopodial F-actin cortex.

In addition, RapB is expression maximal during the early and end stage of development. These results suggest that RapB plays at early and end stage of development in plasma membrane.

67

Interestingly, the roles of RapC seem to be opposite to those of RapB and Rap1. The results demonstrate that RapC is negative plays for cell spreading and cell-substrate adhesion and involved in reorganizing cytokinesis and has a positive impact cell migration and development. Cell lacking RapC (*rapC* null cells) showed increased cell size and cell-substrate adhesion. GFP-RapC-overexpressing cells (GFP-RapC cells) had significantly decreased cell size and cell-substrate adhesion compared to wild-type cells. Unexpectedly, *rapC* null cells caused cytokinesis defects, opposite RapC-overexpressing cells showed normal cytokinesis as wild-type cells. These results suggest that RapC is required for cytoskeleton and cytokinesis. *rapC* null cells caused severe defects in development. When deprived of nutrients, *rapC* null cells shouted delayed cellular aggregation. In addition, *rapC* null cells developed unusual fruiting body as a result of unusual electrotaxis. These results suggest that RapC is required for cell migration or development. Thus, during normal development of *Dictyostelium* cells, I results suggest that RapC should be maintained at proper levels at the aggregation stage of development.

GFP-fusion RapC cells appears to localize to the plasma membrane. In chemotaxing cells, GFP-RapC showed immediately posterior to the leading edge and opposite rear of the cell disappeared. I results suggest that active-RapC is absent from the domain immediately posterior to the leading edge, presumably because the endosomal membrane fraction is excluded by the pseudopodial F-actin cortex.

In addition, RapC is expressed maximal during the late aggregation stage and maintain until fruiting body formation. These results suggest that RapC plays at e late aggregation stage and maintain until fruiting body formation in plasma membrane.

In conclusion, RapB may inhibit cell migration and development. On the other hand, RapC may increase cell migration and development. In addition, RapC has a function opposite to Rap1 and RapB, which should be tumor suppress and tumor promoter relationships.

Conclusions

Calcium ions are involved in the regulation of diverse cellular processes. Fourteen genes encoding calcium binding proteins have been identified in *Dictyostelium*. The present study, suggest that CBP7 is required for cell spreading and cell-substrate adhesion and has a negative impact on development, possibly by inhibiting chemoattractant-directed cell migration. In addition, all of CBP7 EF-hand domains were important for CBP7 to function in the developmental process. CBP7 functions at 6 to 10 hr of developmental stages in the cytosol. Yeast two-hybrid experiments using CBP7 as a bait showed that CBP7 binds to RasG. Characterization of CBP7 in this study will contribute to understanding the functions of calcium signaling and Ras signaling pathway.

Cell movement is a coordinated process of F-actin-mediated protrusions at the leading edge and myosin-mediated contraction of the rear of a cell. The small GTPase Rap1 is involved in the dynamic control of cellular processes, integrin-mediated cell adhesion, and cell migration in *Dictyostelium*. I investigated the roles of RapB and RapC, has high homology group with Rap1. The results indicate that RapB is required for cell spreading and cell-substrate adhesion and has a negative impact on development, possibly inhibition of cell migration through strong cell-substrate adhesion in development. In addition, RapB functions at of developmental stages in membranes, including the ER and endosomal membranes. This study demonstrated that RapC is required for cytoskeleton reorganization, cytokinesis and cell-substrate adhesion and has a positive effect on development, possibly by increasing of cell migration during development. In addition, RapC functions at 10 to 14 hr of developmental stages in membranes, including the ER and endosomal membranes. This study will provide further insight into the molecular mechanisms through which RapB and RapC controls cell adhesion during chemotaxis and development.

References

Andre, B., Noegel, A.A. and Schleicher, M. (1996) *Dictyostelium* discoideum contains a family of calmodulin-related EF-hand proteins that are developmentally regulated. *FEBS Lett* **382**, 198-202.

Catalano, A. and O'Day, D.H. (2013) Rad53 homologue forkhead-associated kinase A (FhkA) and Ca^{2+}-binding protein 4a (CBP4a) are nucleolar proteins that differentially redistribute during mitosis in *Dictyostelium*. *Cell Div* **8**, 4.

Chin, D. and Means, A.R. (2000) Calmodulin: a prototypical calcium sensor. *Trends Cell Biol* **10**, 322-328.

Chisholm, R.L. and Firtel, R.A. (2004) Insights into morphogenesis from a simple developmental system. *Nat Rev Mol Cell Biol* **5**, 531-541.

Clapham, D.E. (2007) Calcium signaling. *Cell* **131**, 1047-1058.

Dharamsi, A., Tessarolo, D., Coukell, B. and Pun, J. (2000) CBP1 associates with the *Dictyostelium* cytoskeleton and is important for normal cell aggregation under certain developmental conditions. *Exp Cell Res* **258**, 298-309.

Dorywalska, M., Coukell, B. and Dharamsi, A. (2000) Characterization and hetereologous expression of cDNAs encoding two novel closely related Ca^{2+}-binding proteins in *Dictyostelium* discoideum. *Biochim Biophys Acta* **1496**, 356-361.

Evans, J.H. and Falke, J.J. (2007) Ca^{2+} influx is an essential component of the positive-feedback loop that maintains leading-edge structure and activity in macrophages. *Proc Natl Acad Sci U S A* **104**, 16176-16181.

Gifford, J.L., Walsh, M.P. and Vogel, H.J. (2007) Structures and metal-ion-binding properties of the Ca^{2+}-binding helix-loop-helix EF-hand motifs. *Biochem J* **405**, 199-221.

70

Jeon, T.J., Lee, D.J., Lee, S., Weeks, G. and Firtel, R.A. (2007a) Regulation of Rap1 activity by RapGAP1 controls cell adhesion at the front of chemotaxing cells. *J Cell Biol* **179**, 833-843.

Jeon, T.J., Lee, D.J., Merlot, S., Weeks, G. and Firtel, R.A. (2007b) Rap1 controls cell adhesion and cell motility through the regulation of myosin II. *J Cell Biol* **176**, 1021-1033.

Jeon, T.J., Lee, S., Weeks, G. and Firtel, R.A. (2009) Regulation of *Dictyostelium* morphogenesis by RapGAP3. *Dev Biol* **328**, 210-220.

Lee, C.H., Jeong, S.Y., Kim, B.J., Choi, C.H., Kim, J.S., Koo, B.M., Seok, Y.J., Yim, H.S. and Kang, S.O. (2005) *Dictyostelium* CBP3 associates with actin cytoskeleton and is related to slug migration. *Biochim Biophys Acta* **1743**, 281-290.

Lee, M.R. and Jeon, T.J. (2012) Cell migration: regulation of cytoskeleton by Rap1 in *Dictyostelium* discoideum. *J Microbiol* **50**, 555-561.

Lusche, D.F., Wessels, D. and Soll, D.R. (2009) The effects of extracellular calcium on motility, pseudopod and uropod formation, chemotaxis, and the cortical localization of myosin II in *Dictyostelium* discoideum. *Cell Motil Cytoskeleton*.

Malchow, D., Mutzel, R. and Schlatterer, C. (1996) On the role of calcium during chemotactic signalling and differentiation of the cellular slime mould *Dictyostelium* discoideum. *Int J Dev Biol* **40**, 135-139.

Mishig-Ochiriin, T., Lee, C.H., Jeong, S.Y., Kim, B.J., Choi, C.H., Yim, H.S. and Kang, S.O. (2005) Calcium-induced conformational changes of the recombinant CBP3 protein from *Dictyostelium* discoideum. *Biochim Biophys Acta* **1748**, 157-164.

Mun, H., Lee, M.R. and Jeon, T.J. (2014) RapGAP9 regulation of the morphogenesis and development in *Dictyostelium*. *Biochem Biophys Res Commun* **446**, 428-433.

Myre, M.A. and O'Day, D.H. (2004) *Dictyostelium* calcium-binding protein 4a interacts with nucleomorphin, a BRCT-domain protein that regulates nuclear number. *Biochem Biophys Res Commun* **322**, 665-671.

71

Rot, G., Parikh, A., Curk, T., Kuspa, A., Shaulsky, G. and Zupan, B. (2009) dictyExpress: a *Dictyostelium* discoideum gene expression database with an explorative data analysis web-based interface. *BMC Bioinformatics* **10**, 265.

Sakamoto, H., Nishio, K., Tomisako, M., Kuwayama, H., Tanaka, Y., Suetake, I., Tajima, S., Ogihara, S., Coukell, B. and Maeda, M. (2003) Identification and characterization of novel calcium-binding proteins of *Dictyostelium* and their spatial expression patterns during development. *Dev Growth Differ* **45**, 507-514.

Siu, C.H., Sriskanthadevan, S., Wang, J., Hou, L., Chen, G., Xu, X., Thomson, A. and Yang, C. (2011) Regulation of spatiotemporal expression of cell-cell adhesion molecules during development of *Dictyostelium* discoideum. *Dev Growth Differ* **53**, 518-527.

Tanaka, Y., Itakura, R., Amagai, A. and Maeda, Y. (1998) The signals for starvation response are transduced through elevated $[Ca^{2+}]i$ in *Dictyostelium* cells. *Exp Cell Res* **240**, 340-348.

Yumura, S., Furuya, K. and Takeuchi, I. (1996) Intracellular free calcium responses during chemotaxis of *Dictyostelium* cells. *J Cell Sci* **109 (Pt 11)**, 2673-2678.

72

국문초록

Dictyostelium 세포이동과 발생과정에서의 CBP7과 Rap 단백질들의 역할

박 병 규

지도교수 : 전 택 중

생명과학과

조선대학교 대학원

칼슘 이온은 다양한 세포 과정 조절에 관여한다. Dictyostelium 에는 칼슘 결합 단백질을 코딩 하는 14 개의 유전자가 알려져 있다. 14 개 CBP 중 하나 인 CBP7 은 169 개의 아미노산으로 구성되어 있으며 4 개의 EF-hand 모티브를 포함하고 있다. Dictyostelium 세포이동과 발생과정에서의 CBP7 의 역할을 조사를 하였고, 연구결과 높은 수준의 CBP7 발현은 발달과정 중 주화성 세포이동을 억제함으로써 발달과정 중 세포 응집에 부정적인 영향을 미친다는 것을 발견하였다. cbp7 null 세포는 야생형 세포와 유사한 주화성 세포이동이 나타났지만, CBP7 과발현 세포는 cAMP 농도가 증가하는 방향으로 주화성 세포이동의 능력이 완전히 잃었다. 이것은 발달과정 동안 다세포발달을 형성하는데 필요한 세포응집 과정의 억제를 가져왔을 것이다. CBP7 과발현한 세포에서는 세포질에 존재하는 칼슘의 농도가 낮은 것으로 관찰되었는데, 이는 주화성 세포이동 결함의 원인이 될 가능성이 높았다고 생각된다. 또한 CBP7 이 세포의 펼쳐짐과 세포-바닥간의 접착에 중요한 역할을 한다는 것을 보여주었다.

cbp7 null 세포는 야생형과 비교했을 때 감소 된 세포 크기와 약한 세포-바닥간의 접착력을 나타났다. 반대로, CBP7 과발현 세포는 야생형과 비교했을 때 평평하고 형태가 넓어지며 강한 세포-바닥간의 접착력을 보였다. 점 돌연변이를 시킨 CBP7 단백질을 이용한 실험결과, CBP7 의 모든 EF-hand 도메인이 CBP7 의 발달 과정에서 기능을 하는데 중요하다는 것을 보여 주었고, CBP7 을 미끼로 사용하는 yeast two-hybrid 실험한결과 CBP7 이 RasG 와 특이적으로 결합한다는 것을 보여 주었다. 이러한 결과는 CBP7 이 모든 EF-hand 도메인을 통한 발달 과정과 RasG 에 결합 함으로써 중요한 역할을 한다는 것을 시사한다. 본 연구는 세포 이동과 발달의 조절에서 칼슘 신호 전달의 역할을 더 잘 이해하는데 기여한다. 또한, 칼슘/Ras 신호전달 경로의 연관성을 이해하는데 기여할 것이다.

Ras 단백질은 증식, 세포 이동, 분화 및 세포 사멸을 비롯한 수많은 세포 신호 전달 경로의 중요한 조절자로 작용하는 작은 단량체인 GTPase 이다. 발달 및 세포 이동에서 Ras 단백질 대부분은 기능이 아직 알려지지 않았다. 그래서 세포 이동 및 발달에서 RapB 및 RapC 의 역할에 대해 조사했다. RapB 와 RapC 는 세포 부착과 세포 이동의 중요한 조절 인자 인 Rap1 와 높은 상 동성(각각 86.6 %, 50.9 %의 아미노산 동일성)을 가졌다. RapB 의 기능을 연구하기 위해서, constitutively active 형태인 세포와(GFP-RapB^{G31V} 세포) dominantly negative 형태인 세포(GFP-RapB^{S36N} 세포)를 준비하고 나서 GFP-RapB^{S36N} 세포의 크기와 세포-바닥간의 접착력이 야생형보다 감소하는 것을 발견했다. 이러한 결과는 RapB 는 세포의 펼쳐짐과 세포-바닥판의 부착력에 긍정적인 역할을 한다는 것을 증명한다. 또한, *Dictyostelium* 세포의 발달과 세포 이동에서의 RapB 의 역할을 조사하였고 GFP-RapB^{G31V} 세포는 발달과정 중 세포 응집에

76

부정적인 영향을 미친다는 것을 발견하였다. 연구결과 발달과정 중 주화성에 의해 세포가 이동 하는 것이 강한 세포-바닥간의 부착에 의해 억제가 나타났을 것이라고 생각한다. 이러한 결과는 RapB 가 세포 이동과 발달에 부정적인 역할을 한다는 것을 보여준다.

RapC 의 기능을 조사하기 위해서, 상동재조합에 의해 RapC 가 없는 세포를 준비하였다. 놀랍게도 RapC 는 Rap1 및 RapB 와는 반대되는 기능을 한다는 것을 확인하였다. *rapC* null 세포는 야생형에 비교했을 때 평평해지고 펴져있는 형태를 가지고 세포-바닥판의 부착력이 강하게 나타났다. 이러한 결과는 RapC 는 Rap1 과 RapB 와 반대 역할로 세포의 퍼짐과 세포-바닥판의 부착력에 부정적인 역할을 한다는 것을 입증하였다. 또한, *rapC* null 세포는 cytokinesis 결함이 있었다. *rapC* null 세포의 이러한 특징은 GFP-RapC 를 과발현 함으로써 회복되었다. 이러한 실험결과는 RapC 가 cytokinesis 에 필요하다는 것을 보여주었다. *Dictyostelium* 세포의 발달과 세포이동에 관한 RapC 의 역할을 조사하였고, *rapC* null 세포는 발달과정 중 세포 응집과 자실체 형성에 부정적인 영향을 미친다는 것을 발견하였다. 연구결과 발달과정 중 주화성에 의해 세포가 이동하는 것이 강한 세포-바닥간의 부착에 의한 억제와 전기자극에 대한 세포이동 결함으로 나타났다. 실험결과는 RapC 가 Rap1 과 RapB 와는 반대로 세포 이동 및 발달에 긍정적인 역할을 한다는 것을 보여주었다.

위치조사는 RapB, RapC 가 세포원형질막에 국한된 것으로 보이고, 이동하는 세포에서는 즉각적으로 세포의 앞쪽 가장자리에 나타남을 보여주었다.

본 연구는 *Dictyostelium* 에서 세포 골격의 재 배열과 형태 형성을 조절하는 Rap 단백질들의 분자 메커니즘에 대한 이해를 제공하는데 기여한다.

77